Development 140, 552-561 (2013) doi:10.1242/dev.085621

Neural development is dependent on the function of specificity protein 2 in cell cycle progression

Huixuan Liang[1], Guanxi Xiao[1], Haifeng Yin[1], Simon Hippenmeyer[2], Jonathan M. Horowitz[1] and H. Troy Ghashghaei[1,*]

SUMMARY

Faithful progression through the cell cycle is crucial to the maintenance and developmental potential of stem cells. Here, we demonstrate that neural stem cells (NSCs) and intermediate neural progenitor cells (NPCs) employ a zinc-finger transcription factor specificity protein 2 (Sp2) as a cell cycle regulator in two temporally and spatially distinct progenitor domains. Differential conditional deletion of Sp2 in early embryonic cerebral cortical progenitors, and perinatal olfactory bulb progenitors disrupted transitions through G1, G2 and M phases, whereas DNA synthesis appeared intact. Cell-autonomous function of Sp2 was identified by deletion of Sp2 using mosaic analysis with double markers, which clearly established that conditional *Sp2*-null NSCs and NPCs are M phase arrested *in vivo*. Importantly, conditional deletion of Sp2 led to a decline in the generation of NPCs and neurons in the developing and postnatal brains. Our findings implicate Sp2-dependent mechanisms as novel regulators of cell cycle progression, the absence of which disrupts neurogenesis in the embryonic and postnatal brain.

KEY WORDS: Neurogenesis, Neural stem cells, Neural progenitors, Sp2, Cell cycle, M phase, Mouse

INTRODUCTION

The functioning of neural stem cells (NSCs) and intermediate progenitors (NPCs) is crucial to embryonic and postnatal development of the central nervous system (CNS) (Guillemot, 2007; Pinto and Götz, 2007; Kriegstein and Alvarez-Buylla, 2009; Okano and Temple, 2009). NSCs continuously self-renew and expand in the ventricular zones (VZ) of the early embryonic neuroectoderm and maintain their population during early CNS development (Götz and Huttner, 2005). Shortly after specification of the neuroectoderm, NSCs give rise to NPCs, which begin their neurogenic divisions to generate various types of neurons that occupy the CNS (Kriegstein and Alvarez-Buylla, 2009; Costa et al., 2010). Division of NPCs largely occurs in various subventricular zones (SVZ) in the embryonic brain (Noctor et al., 2004; Miyata et al., 2004; Haubensak et al., 2004; Pontious et al., 2008). Whereas the vast majority of progenitor domains in the CNS become dormant by birth, the subependymal zone (SEZ) of the lateral ventricles and the rostral migratory stream (RMS) continue to harbor NSCs and NPCs in postnatal and adult mice (Doetsch et al., 1999a). The postnatal NSCs and NPCs give rise to neuroblasts that migrate via the RMS to the olfactory bulbs where they differentiate into interneurons.

It is well established that maintenance of a delicate balance between proliferative and neurogenic divisions in NSCs and NPCs is a key determinant for appropriate production and specification of neurons (Götz and Huttner, 2005; Farkas and Huttner, 2008). Key regulators of this balance include intrinsic and extrinsic signals that impact cell polarity, adherent junctions, centrosomal functions and transcriptional regulation (Fietz and Huttner, 2011). Moreover, several cell cycle regulators have emerged as important players in maintaining the balance between proliferative and neurogenic divisions in NSCs and NPCs (e.g. Calegari et al., 2005; Arai et al., 2011; Gruber et al., 2011; García-García et al., 2012). Cell cycle regulators form complex signaling networks that drive progression through phases of the cell cycle, and ultimately affect the length and integrity of mitosis. Understanding how distinct cell cycle regulators impact the shift from expansion and self-renewal to neurogenesis in NSCs and NPCs is important for strategies in cellular reprogramming (Singh and Dalton, 2009) and understanding many neurodevelopmental disorders (Manzini and Walsh, 2011).

The specificity protein (Sp) family of transcription factors has been associated with progenitor functions, including regulation of the cell cycle (Marin et al., 1997; Black et al., 2001; Krüger et al., 2007; Baur et al., 2010). Although Sp family members are co-expressed broadly, developmental defects exhibited by subtype-specific knockout mice indicate that their functions may only partially overlap (Supp et al., 1996; Marin et al., 1997; Bouwman et al., 2000; Nguyên-Trân et al., 2000; Göllner et al., 2001; van Loo et al., 2003). Recent studies indicate Sp2 is required for early embryonic development in mice and zebrafish (Baur et al., 2010; Xie et al., 2010), and Sp2 overexpression in skin stem cell and progenitor populations is oncogenic (Kim et al., 2010). Acute loss of Sp2 negatively regulates the proliferation of immortalized mouse fibroblasts (Baur et al., 2010). Moreover, whether Sp2 functions as a bona fide transcription factor has remained unclear; past reports have indicated that Sp2 has little, if any, transcriptional activity or DNA-binding capacity in mammalian cells (Moorefield et al., 2004), whereas a recent report claims widespread DNA binding to regulatory regions of a wide range of vital genes (Terrados et al., 2012). Regardless, the cell biological relevance of Sp2 has remained uncertain. Here, we report that Sp2 is a key regulator of progression through the cell cycle in NSCs and NPCs. Moreover, conditional deletion of Sp2 in the brain severely impacts neurogenesis in both embryonic and postnatal CNS.

[1]Department of Molecular Biomedical Sciences and Center for Comparative Medicine and Translational Research, College of Veterinary Medicine, North Carolina State University, Raleigh, NC 27607, USA. [2]Institute of Science and Technology Austria, Am Campus 1, A-3400 Klosterneuburg, Austria.

*Author for correspondence (troy_ghashghaei@ncsu.edu)

Accepted 15 November 2012

MATERIALS AND METHODS

Animals

Animals were used under Institutional Animal Care and Use Committee and North Carolina State University regulations. *Sp2* floxed mice were generated using homologous recombination. The targeting vector included a 3.2-kb genomic region corresponding to exons 3 and 4 of the *Sp2* gene flanked by two loxP sites. A 1.8-kb genomic fragment upstream of exons 3 corresponded to the small arm, and included neomycin-resistance for positive selection, which was removed by flipase treatment recognized by the Frt sites flanking the cassette. For negative selection, a PGK-tk:HSV cassette was inserted outside the region of gene homology. The targeting construct was electroporated into mouse129 ES cells, which were then positively and negatively selected. Genomic DNA derived from surviving ES cells was analyzed by PCR, Southern blotting and DNA sequencing. Confirmed ES cells were microinjected into the C57BL/6 blastocysts and implanted into pseudo-pregnant females. Chimeric pups were identified by coat color, germ line transmission, PCR and Southern blotting. *Sp2* deleted floxed alleles were detected by PCR using the following primers: SAF-3, 5′-GAGATTCAGATTTAGAGGGCTACCAGTGTCCA-3′; and TAR-2, 5′-CGCTCAAGCCCCATTGCTGGGCCTGGTGACAA-3′.

To conditionally delete Sp2 in NSCs and NPCs *Sp2* floxed mice were crossed to transgenic *Nestin-cre* and knock-in *Emx1*^{cre} mice, both of which were on cre-responsive reporter *tdTomato* (tdTom) to track cre-mediated recombination (Jackson Laboratories; supplementary material Table S1). For mosaic analyses, *MADM11-GT/TG:Sp2* $^{F/+}$*:Nestin-cre* mice were generated using breeding schemes previously described (Hippenmeyer et al., 2010).

For fixed tissue analyses, mice were sacrificed at multiple developmental stages by Avertin overdose (7.5 mg/g body weight) followed by transcardial perfusion with 4% formaldehyde.

BrdU and IdU administration

Mice at various developmental stages were administered intraperitoneal injections of bromodeoxyuridine (BrdU) or iodinated deoxyuridine (IdU) (Sigma) at 100 µg/g body weight. For pulse-chase experiments, a single pulse of BrdU was followed by sacrifice at 1, 4 and 12 hours after the last BrdU injection. For assessment of cell cycle exiting, three pulses of BrdU were administered at 2-hour intervals, and injected mice were perfused 48 hours after the last pulse. For estimation of the cell cycle duration, BrdU/IdU dual labeling was performed as described previously (Martynoga et al., 2005).

Tissue processing and cell counting

Following perfusion, brains were removed and sectioned using a vibratome, and floating sections were immunohistochemically processed using standard procedures. For *in situ* hybridization and fluorescence *in situ* hybridization, an Sp2-specific probe was generated and used for tissue staining as described before (Yin et al., 2010). Cell numbers and densities were quantified using standard stereological estimation methods as described previously (Jacquet et al., 2009a; Jacquet et al., 2009b). Significance was determined using Student's *t*-test and all values were expressed as mean±s.e.m. See supplementary material Table S2 for details.

Electroporation, tissue culture and neurosphere assay

Ex utero electroporation was performed in decapitated embryonic brains as previously described before (Hand et al., 2005). Two µl of a *pCAG-cre* plasmid (4 µg/µl; Addgene) was injected into the lateral ventricles of isolated embryonic heads followed by electroporation. Organotypic slices were obtained and cultured as previously described (Jacquet et al., 2010). Neurosphere growth and differentiation assays were performed as previously described (Jacquet et al., 2009b).

Flow cytometry and cell sorting

SEZ and RMS regions were microdissected followed by single cell enzymatic dissociation. Cells were then washed with 5 ml cold 0.1 M PBS and fixed with 5 ml 70% ethanol. After fixation, cells were washed with 5 ml cold 0.1 M PBS and then stained at room temperature for 45 minutes with a solution containing propidium iodide (1 µg/ml; Sigma) and RNase A (1 mg/ml; Roche). Isolated SEZ and RMS cells were sorted or analyzed for DNA content by flow cytometry at the Flow Cytometry and Cell Sorting core facility at the College of Veterinary Medicine at North Carolina State University (Raleigh, NC, USA). For fluorescence-activated

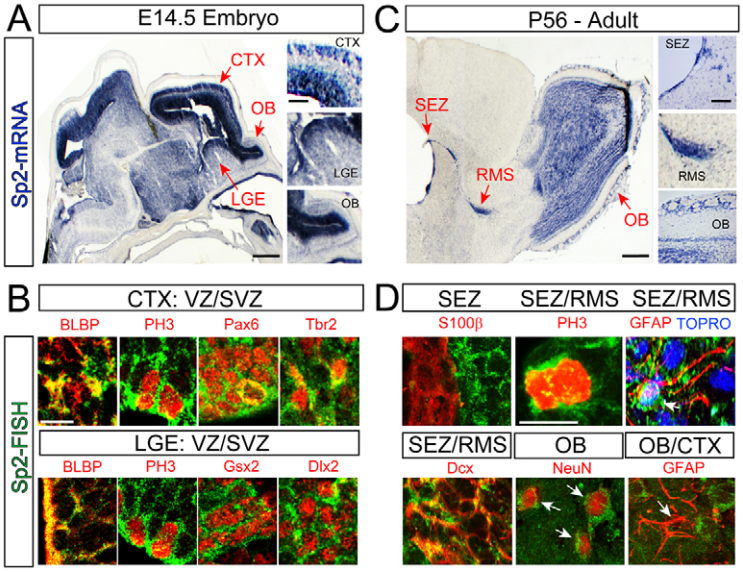

Fig. 1. Sp2 expression in the brain. (**A**) *In situ* hybridization using a probe specific to the full-length transcript of Sp2 revealed high expression in the germinal zones of the E14.5 cerebral cortex (CTX), lateral ganglionic eminence (LGE) and olfactory bulb (OB). (**B**) Fluorescence *in situ* hybridization using the Sp2 probe (green) co-labeled with antibodies (red) against BLBP, PH3 and Pax6 in the VZ, and Tbr2 in the SVZ. Similar specificity for Sp2 expression was seen in the LGE where the labeled transcript overlapped with BLBP+, PH3+ and Gsx2+ progenitors in the VZ, and with Dlx2+ progenitors in the SVZ. (**C**) *In situ* hybridization for Sp2 in the P56 young adult brain revealed restricted expression in neurogenic regions, including the subependymal zone (SEZ), rostral migratory stream (RMS) and OB. (**D**) Fluorescence *in situ* hybridization characterization of Sp2+ cell types in the SEZ, RMS and OB. Sp2 mRNA (green) overlapped with cells labeled for PH3 and Dcx (red), which label mitotic progenitors and migrating neuroblasts in the SEZ and RMS, respectively. Subsets of neurons in the granule cell layer of the OB (NeuN+, red) also expressed Sp2. Ependymal cells labeled with S100β antibody (red) and parenchymal astrocytes labeled with GFAP antibody (red) largely failed to overlap with Sp2 mRNA. Scale bars: 200 µm in A,C; 60 µm in A,C (insets); 5 µm in B,D (bar in BLBP applies to all except PH3 in D).

cell sorting (FACS), single cell suspensions harvested from SEZ and RMS regions of mice on the MADM11 background were sorted using a Dako Cytomation MoFlo high speed machine.

Western blotting

SEZ and RMS cells from conditional control mice (cWT) and Nestin:cKO brains were lysed followed by homogenization. Total proteins were denatured and samples were boiled and ran on a reducing SDS-PAGE gel followed by transfer to nitrocellulose membrane. Membranes were labeled and developed using standard methods.

RESULTS

Sp2 is expressed by embryonic and postnatal NSCs and NPCs

In situ hybridization of the embryonic CNS revealed robust expression in germinal layers of the E14.5 embryo. Particularly strong expression was detected in the ventricular zones (VZ) and subventricular zones (SVZ) of the entire CNS, including the neocortex, the lateral ganglionic eminence (LGE) and the olfactory bulb (OB; Fig. 1A). To determine the cell specificity of Sp2 mRNA expression, we conducted fluorescence *in situ* hybridization in combination with immunohistochemistry for various cell types in the E14.5 cortex and LGE (Fig. 1B). The strongest expression was seen in mitotic progenitors expressing the phosphorylated form of Histone H3 (PH3) in the VZ and SVZ of both progenitor domains (Fig. 1B). Correspondingly, VZ progenitors in the cerebral cortices immunoreactive for paired box gene 6 (Pax6) and for genetic screened homeobox 2 (Gsx2) in the LGE both expressed Sp2. Basal NPCs expressing T-box brain gene 2 (Tbr2; Eomes – Mouse Genome Informatics) in the cortex, and LGE-specific NPCs expressing distalless homeobox 2 (Dlx2) also expressed Sp2. Thus, Sp2 expression largely and ubiquitously overlapped with NSCs and NPCs in the embryonic CNS.

Sp2 expression continued after birth only in structures that remain neurogenic during postnatal and adult periods, including the SEZ, RMS and the olfactory bulb (OB; Fig. 1C), as well as the granule layers in the cerebellum and hippocampus (supplementary material Fig. S1). Fluorescence *in situ* hybridization analysis in the SEZ and RMS of young adult (P56) mice indicated that Sp2 mRNA largely overlapped with cells within the cell cycle (e.g. PH3+), migrating neuroblasts expressing doublecortin (Dcx) and a small fraction of astrocytes positive for the glial fibrillary acid protein (GFAP+; Fig. 1D). Ependymal cells labeled with S100β, which are postmitotic and do not proliferate, were devoid of Sp2 mRNA (Fig. 1D). Sp2 was also expressed at low levels by some granule neurons in the olfactory bulbs (Fig. 1D) and in the hippocampus and cerebellum (supplementary material Fig. S1). Thus, Sp2 is primarily expressed in NSCs, NPCs and migrating cells within the germinal zones of the embryonic and adult brains, which suggested a potential role for Sp2 in cell cycle regulation.

Nestin-cre mediated deletion of *Sp2* results in defective proliferation of postnatal NSCs and NPCs

To determine whether or not Sp2 expression is required for cellular and tissue development in the CNS, we adopted a loss-of-function approach via the conditional deletion of Sp2 in the CNS. Mice carrying 'floxed' Sp2 alleles were generated and crossed to a transgenic line of *Nestin-cre* mice to direct cre-mediated recombination to neuronal progenitors (Fig. 2A; supplementary material Fig. S2). Mice with genotypes *Nestin-cre:Sp2*$^{+/+}$, *Sp2*$^{F/+}$ and *Sp2*$^{F/F}$ served as conditional controls (cWT); *Nestin-cre:Sp2*$^{F/+}$ were conditional heterozygous

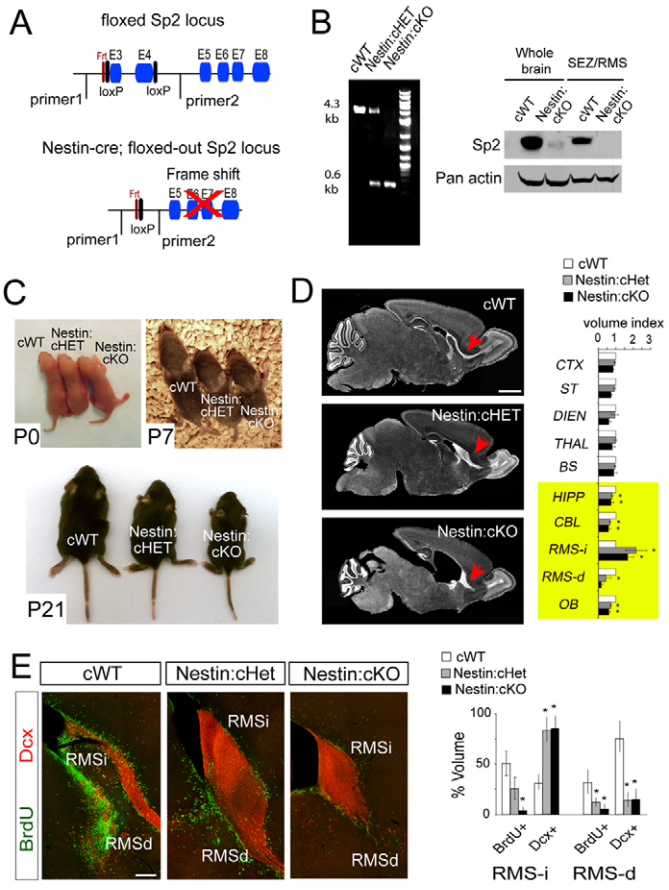

Fig. 2. *Nestin-cre* driven conditional deletion of Sp2 disrupts the postnatal stem cell niche. (**A**) *Sp2* 'floxed' mice crossed to *Nestin-cre* transgenic mice to delete exons 3 and 4, and prevent transcription of Sp2 due to a frame shift. (**B**) PCR analysis of genomic DNA derived from P21 Nestin:cHet and Nestin:cKO brains using primer1 and primer2 indicated in A. Undeleted floxed allele yielded a 4.3 kb PCR product, whereas the deleted allele was 0.6 kb in size. Western blotting against Sp2 in protein extracts from whole brains or from microdissected SEZ/RMS obtained from P0 mice indicated near complete absence of Sp2 in the Nestin:cKO brains. (**C**) Nestin:cHet and Nestin:cKO mice appeared normal at birth (P0), but failed to grow during early postnatal life (e.g. at P7 and P21) compared with littermate cWT controls. (**D**) Nissl-stained sagittal sections revealed ectopic cellular accumulations in the P21 SEZ and RMS of both Nestin:cHet and Nestin:cKO mice (red arrows). Volume indices, calculated using stereological estimation methods, indicated significant reductions in the volumes of the Nestin:cHet and Nestin:cKO OB, hippocampal formation (HIPP) and cerebellum (CBL). Significant expansions were noted in the initial segment of the RMS (RMS-i) in both Nestin:cHet and Nestin:cKO brains. (**E**) Confocal micrographs of Dcx-labeled neuroblasts (red) and BrdU incorporated cells (green) in P21 RMS-i and RMS-d. The expanded region in RMS-i was largely occupied by Dcx+ migrating neuroblasts in Nestin:cHet and Nestin:cKO brains, but the number of BrdU+ proliferating cells was significantly decreased throughout the RMS regions. Data are mean±s.e.m.; *P<0.01, Student's t-test, n=3/age group. Scale bars: 300 μm in D; 100 μm in E.

(Nestin:cHet); and *Nestin-cre:Sp2*$^{F/F}$ were conditional homozygous (Nestin:cKO) Sp2 'knockout' mice. Mendelian distribution of the Nestin:cHet and Nestin:cKO progeny analyzed in 203 pups from 22 litters appeared normal at birth (P=0.82 from χ^2 test; supplementary material Fig. S2). Near complete deletion

of *Sp2* was confirmed by PCR analysis of genomic DNA and protein extracts from P21 Nestin:cKO brains (Fig. 2B).

Despite an apparently normal embryonic development, Nestin:cHet and Nestin:cKO mice grew more slowly during postnatal stages when compared with cWT littermates (Fig. 2C). Although Nestin:cHet animals thrived akin to cWT littermates, many Nestin:cKO mice perished between two and five weeks of age with only a few surviving into adulthood (n=10 Nestin:cKO pups from three independent litters; only three Nestin:cKOs survived beyond 2 months of age). Specific defects within the CNS became apparent during the first 2 weeks of postnatal life and were most profound between postnatal days 7 (P7) and P21 (Fig. 2D). These included mild hydrocephalous in 32% of P21 Nestin:cKO mice (n=28), which indicated potential defects in maintenance of homeostasis in the periventricular tissue of the CNS.

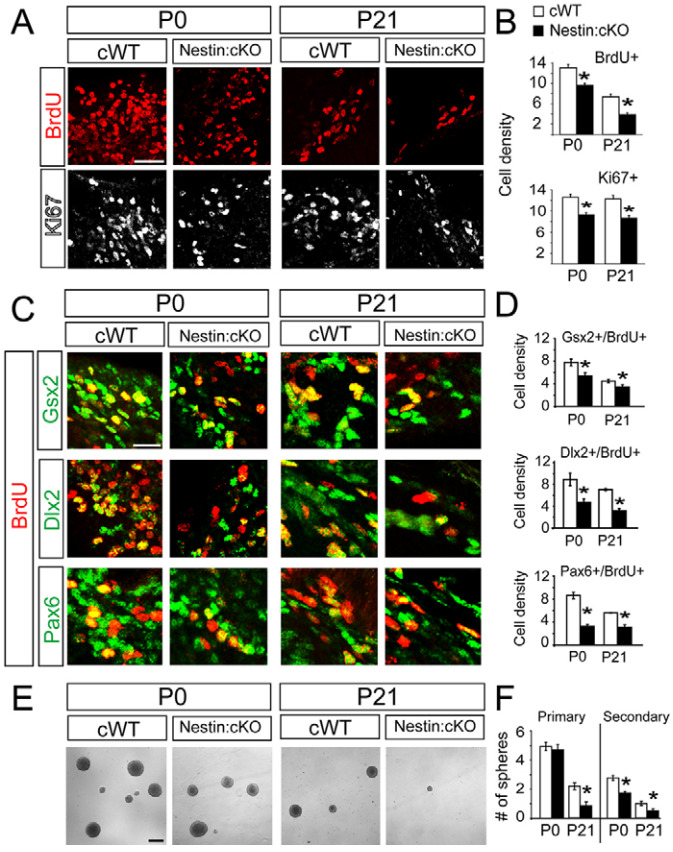

Fig. 3. Aberrant progenitor proliferation in the postnatal *Sp2*-null brain. (**A**) Confocal micrographs of Ki67+ and BrdU+ (red) cycling cells in the P0 and P21 cWT and Nestin:cKO SEZ. (**B**) Quantitative comparison of BrdU+ and Ki67+ cellular densities in the cWT and Nestin:cKO SEZ (number of cells in chart are $\times 10^5$/mm^3). (**C**) The proliferating portions of progenitors expressing the transcription factors Gsx2, Dlx2 and Pax6 were identified by a 1-hour BrdU pulse. Representative confocal photomicrographs illustrating a visible decline in proliferation (BrdU+, red) of progenitor types (green) in the SEZ (Gsx2 and Dlx2 domain) and RMS (Pax6 domain). (**D**) Densities of BrdU+ progenitor types were estimated using stereological methods. Data are mean±s.e.m.; *P<0.01, Student's t-test, n=3/age group. (**E**) Primary neurospheres generated from cWT and Nestin:cKO SEZ and RMS progenitors harvested at P0 and P21. (**F**) Quantification of both primary and secondary neurospheres derived from P21 cWT and Nestin:cKO progenitors. *P<0.05, Student's t-test, n=3/age group. Scale bars: 20 μm in A; 10 μm in C; 200 μm in E.

Stereological estimations of Nissl stained P21 brain sections revealed significant reductions in the volumes of the OB, hippocampus, and cerebellum in Nestin:cHet and Nestin:cKO brains (n=3 per genotype; Fig. 2D). Upon closer examination, the RMS appeared enlarged and marker analysis revealed that the 'bulge' in the Nestin:cHet and Nestin:cKO RMS was largely occupied by Dcx+ neuroblasts (Fig. 2E). These histological defects were never observed in brains from *Nestin-cre: Sp2*$^{+/+}$ (Fig. 2D), *Sp2*$^{F/+}$ or *Sp2*$^{F/F}$ mice (data not shown), demonstrating that the identified morphological phenotypes were independent of potential cre-related or hypomorphic issues.

To determine whether the neuroblast-filled bulges in Nestin:cKO SEZ and RMS corresponded to disruptions in proliferation of NSCs and NPCs, BrdU was administered to P0 and P21 mice followed by 1 hour of survival. Quantification of the number of BrdU+ progenitors (largely S-phase cells after 1 hour), revealed a significant reduction in the SEZ and RMS in both Nestin:cHet and Nestin:cKO brains (Fig. 2E; Fig. 3A). Based on the consistent decline in proliferation of both Nestin:cHet and Nestin:cKO progenitors, we decided to focus on comparing cWT and Nestin:cKO brains hereafter.

The combination of BrdU with the pan cell cycle marker Ki67 indicated an overall reduction in NSC and NPC populations in the Nestin:cKO SEZ and RMS (Fig. 3A,B). We next used progenitor type-specific markers, which revealed a uniform reduction of all cycling populations in the SEZ and RMS of Nestin:cKO brains (Fig. 3C,D). To determine whether the reductions in progenitor cell subsets were cell intrinsic or due to non-autonomous *in vivo* effects, the SEZ and RMS of P0 and P21 cWT and Nestin:cKO brains were microdissected and cultured to generate neurospheres (Reynolds and Weiss, 1992). In line with our *in vivo* findings, the number of both primary and secondary neurospheres from Nestin:cKO progenitors were compromised and progressively worsened between P0 and P21 (Fig. 3E,F). Taken together, these results suggested that Sp2 is an important regulator of proliferation in postnatal NSCs and NPCs.

Notwithstanding the robust expression of Sp2 in all neuronal progenitor domains, we failed to detect significant proliferation phenotypes in embryonic progenitors (Fig. 4A,B). These findings suggested that conditional deletion of Sp2 was tolerated *in utero*, but following additional analyses it became clear that the *Nestin-cre* allele obtained from Jackson laboratory was insufficient to drive recombination in embryonic NSCs and NPCs (Liang et al., 2012). To assess whether embryonic NSCs and NPCs require Sp2 for their proliferation, we expressed cre in *Sp2*$^{F/F}$ and *Sp2*$^{+/+}$ embryonic brains with tdTomato cre recombination reporter (tdTom) by means of *ex utero* electroporation using a *pCAG*-cre construct (Fig. 4C). The brains were harvested and organotypic slices were collected and maintained for two days *in vitro* (E13.5 + 2 DIV; Fig. 4C-E). The cultures were supplemented with BrdU for 1 hour followed by fixation and immunohistochemistry to visualize BrdU+ cells. Cre-mediated recombination in embryonic *Sp2*$^{F/F}$ brains resulted in a significant decrease in the percentage of BrdU+ cells in the tdTom+ population in the VZ and SVZ of the developing cortex (Fig. 4D). These findings led us to conclude that akin to postnatal NSCs and NPCs, the proliferation of embryonic progenitors within the VZ and SVZ is Sp2 dependent.

Sp2 deficiency results in apparent M-phase arrest in NSCs and NPCs

The significant decline in BrdU incorporation in conditional *Sp2-null* NSCs and NPCs suggested potential defects in cell cycle

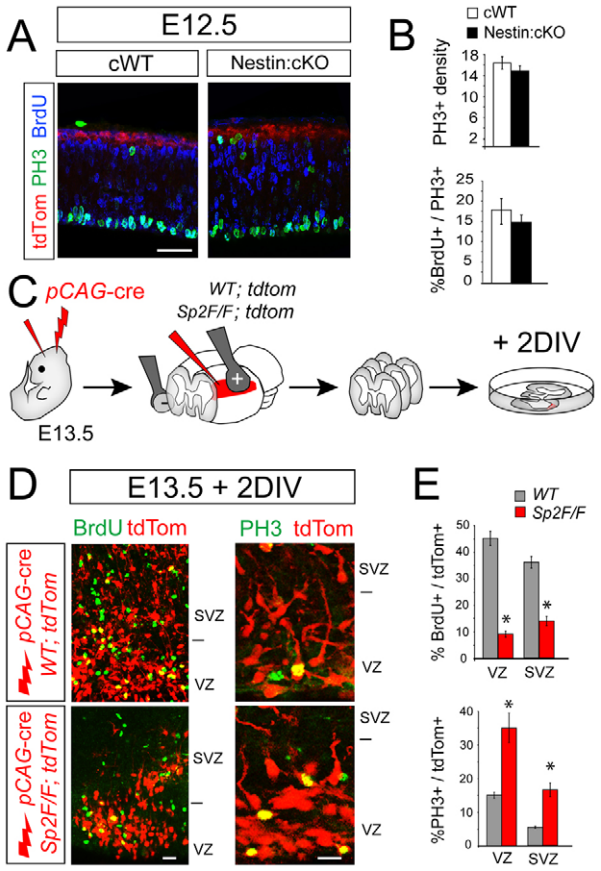

Fig. 4. Sp2 is required for proliferation of embryonic NSCs and NPCs. (**A**) Density of PH3+ (green) and BrdU+ (blue) nuclei was indistinguishable in the developing cortex of Nestin-cre driven cWT and Nestin:cKO brains at E12.5, owing to inefficient recombination (tdTom, red) in the VZ. (**B**) PH3+ densities were obtained in the VZ of Nestin:cKO and cWT mice and are presented as mean±s.e.m. (**C**) *Ex vivo* electroporation of a pCAG-cre construct into the embryonic brains of E13.5 tdTomato (tdTom) reporter mice on a $Sp2^{+/+}$ and $Sp2^{F/F}$ backgrounds. (**D**) tdTom+ cells (red) reported on cre-mediated recombination. Fractions of proliferating tdTom+ cells were determined by staining for BrdU or PH3 (green; BrdU applied to culture bath 1 hour prior to fixation). (**E**) Charts illustrate differences in percentage of tdTom+ cells co-labeled with BrdU and PH3 in the ventricular zone (VZ) and subventricular zone (SVZ) of the developing cerebral cortices. Data are mean±s.e.m. BrdU, **P*<0.01, Student's *t*-test, *n*=3/age group. PH3, **P*<0.05, Student's *t*-test, *n*=3/age group. Scale bars: 20 μm in A; 10 μm in D.

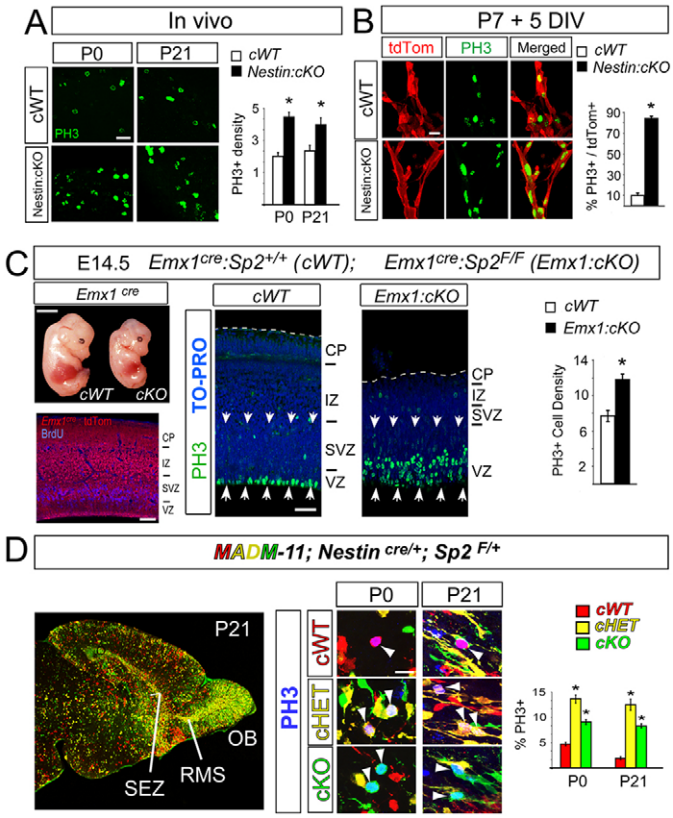

Fig. 5. M-phase arrest in niches of *Sp2*-null NSCs and NPCs. (**A**) Significant increase in density of phospho-histone H3-expressing (PH3+) presumptive M-phase cells (green) in the P0 and P21 Nestin:cKO SEZ and RMS. (**B**) P7 Nestin:cKO SEZ/RMS cells plated on poly-d-lysine for 5 days contained a higher percentage of cells co-labeled with PH3 (green) among the total population of tdTom+ cells. (**C**) E14.5 Emx1:cKO embryos displayed growth retardation compared with littermates. $Emx1^{cre}$ is sufficient in driving recombination in the VZ and SVZ of the embryonic cortex (tdTom, red; BrdU, blue). There were more M-phase (PH3+) cells in the E14.5 Emx1:cKO VZ and SVZ (arrows) compared with the cWT cerebral cortex. (**D**) *In vivo* analysis of *Nestin-cre:*$Sp2^{F/+}$*:MADM-11* progenitors. Percentages of PH3+ (blue) cells that were Nestin:cKO (green) and Nestin:cHet (yellow) were significantly higher than cWT (red) progenitors (PH3+ color labeled cells, arrowhead). Data are mean±s.e.m.; **P*<0.05, Student's *t*-test, *n*=3/age group. Scale bars: 10 μm in A,B,D; 300 μm in C, whole embryo; 40 μm in C, sections.

compartments. Using cell cycle phase-specific markers, we found the percentage of presumptive M-phase cells expressing the phosphorylated form of histone H3 (PH3) was significantly elevated in the VZ and SVZ of embryonic $Sp2^{F/F}$ cortical slices electroporated with pCAG-cre (Fig. 4D,E) and in the SEZ and RMS of postnatal Nestin:cKO mice (Fig. 5A). The elevated levels of PH3 expression appeared cell intrinsic as cultured Nestin:cKO NSCs and NPCs expressed PH3 in significantly higher numbers than control cultures (Fig. 5B), suggesting a potential M-phase arrest in *Sp2*-null progenitors. To obtain an *in vivo* model in which we could sufficiently delete Sp2 in embryonic NSCs and NPCs, we used the well characterized $Emx1^{cre}$ mice to direct Sp2 deletion to the VZ and SVZ of the dorsal telencephalon (Liang et al., 2012). In contrast to the Nestin-cre line, sufficient $Emx1^{cre}$-dependent recombination in the VZ and SVZ was confirmed at E14.5 (tdTom+ cells, red; Fig. 5C) (Liang et al., 2012). Every E14.5 Emx1:cKO cortex exhibited significant increase in density, and profound disruption in organization of PH3+ nuclei in the VZ and SVZ (Fig. 5C, arrows). Thus, *Sp2*-null progenitors appeared arrested in the M phase, concomitant with an overall decline in density of cycling progenitors during embryonic and postnatal periods.

To conclusively exclude potential cell non-autonomous effects of Sp2 deletion *in vivo*, we next used mice that allow for mosaic analysis with double markers through targeted 'MADM' insertions into the 3′ region of chromosome 11 (MADM-11) (Hippenmeyer et al., 2010). As chromosome 11 also carries the *Sp2* gene in mice, progenitors carrying one floxed allele of *Sp2* on the homozygous MADM-11 background will undergo cre-mediated mitotic

recombination, resulting in generation of cWT (tdTom+), Nestin:cHet (GFP+ tdTom+), and Nestin:cKO (GFP+) cells from clones of NSCs and NPCs that label distinctly with fluorescent reporters (Fig. 5D). However, cre-mediated mitotic recombination is not ubiquitous and occurs only in a small fraction of NSCs and NPCs, which allows for mosaic and clonal analysis of progenitor functions in a mixed heterozygous and wild-type background. To confirm that cellular genotypes matched the expected reporter combinations, MADM cells were sorted and subjected to PCR genotyping, which indicated that Sp2 genotypes (i.e. wild type, heterozygous or homozygous) were concordant with the expression of MADM reporters (supplementary material Fig. S3). Subsequent *in vivo* analyses of *Nestin-cre:Sp2$^{F/+}$:MADM-11* progenitors substantiated our findings that the percentages of PH3+ nuclei in Nestin:cKO and Nestin:cHet populations (green and yellow cells, respectively in Fig. 5D) were significantly higher than in the cWT progenitor pool (red cells in Fig. 5D). Thus, the elevated density of PH3+ (presumptive M phase) cells in the absence of Sp2 expression, despite the severe depletion of other proliferation indices, strongly favored a possible defect in cell cycle progression.

Sp2 is required for progression through distinct stages of the cell cycle in NSCs and NPCs

To determine whether cycling progenitor cells were arrested in, or progressed more slowly through, G2/M, a series of *in vivo* BrdU pulse-chase and *in vitro* flow cytometric experiments were conducted on postnatal NSCs and NPCs (Fig. 6A-D; also see supplementary material Fig. S4 for results from P0 brains). To assess the acute effects of Sp2 deletion on the S-to-M transition, a single pulse of BrdU at P0 and P21 was followed by a 1-hour survival time. BrdU labeling was then combined with PH3 immunohistochemistry to detect cells that had undergone S-to-G2/M transition during the 1-hour chase period in both P0 and P21 brains (Fig. 6A; supplementary material Fig. S4). The percentage of BrdU+ cells co-labeled with PH3+ was significantly higher in Nestin:cKO mice at P0 and P21 (Fig. 6A,B, arrows; supplementary material Fig. S4). Thus, BrdU-incorporated nuclei appeared to rapidly transition into M, suggesting that the length of S-to-G2/M transition was shortened in the absence of Sp2.

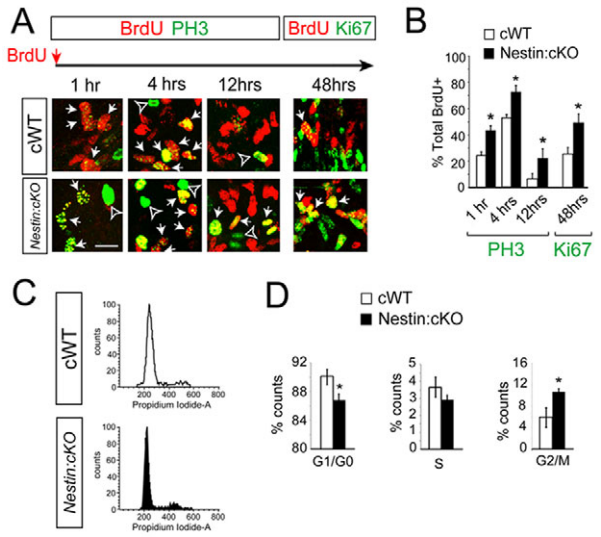

Fig. 6. Analysis of cell cycle progression in Sp2-deficient NSCs and NPCs. (**A**) Cell cycle progression was assessed *in vivo* by means of administering pulses of BrdU followed by different chase periods prior to sacrifice (1 hour, 4 hours, 12 hours and 48 hours; BrdU, red arrow). S-to-M progression was quantified by co-labeling for BrdU (red) and PH3 (green; arrows) or Ki67 (48-hour group, arrows). M-phase cells that did not incorporate BrdU were labeled as PH3+/BrdU negative (arrowheads). (**B**) Nestin:cKO progenitors had a consistent increase in percentage of BrdU+/PH3+ cells over total BrdU+ cells in the 1-hour, 4-hour and 12-hour groups. The percentage of cells remaining or re-entering the cell cycle (BrdU+/Ki67+ cells over total BrdU cells) during the 48-hour chasing period was dramatically increased in Nestin:cKO progenitors. (**C**,**D**) Flow cytometric data from cycling cells harvested from P21 Nestin:cKO SEZ and RMS, illustrating a significantly higher proportion of cells in the G2/M phases and a reduced proportion in G1/G0 phase. Data are mean±s.e.m.; **P*<0.05, Student's *t*-test, *n*=3/age group. Scale bar: 10 μm.

Next, to determine whether the transition defect in *Sp2*-null NSCs and NPCs was due to changes in S-phase duration or to faulty G2/M progression, the length of S-phase was determined by a single pulse of IdU followed by a pulse of BrdU 3 hours later (see supplementary material Fig. S5). Double labeling for BrdU and IdU and estimation of S-phase length failed to distinguish Nestin:cWT and Nestin:cKO NSCs and NPCs (supplementary material Fig. S5). This finding suggested that the duration of S phase was independent of Sp2 expression, and that the length of the G2-M transition was shortened.

To gain more insight into the fate of *Sp2*-null cycling cells that transitioned into M rapidly, we extended the survival time to 4 hours which still yielded a higher percentage of BrdU+ PH3+ NSCs and NPCs in Nestin:cKO brains (Fig. 6A,B; supplementary material Fig. S4). In addition, a significant fraction of PH3+ cells in the Nestin:cKO SEZ and RMS remained BrdU negative (Fig. 6A, arrowheads; supplementary material Fig. S4), suggesting that *Sp2*-null progenitors may be arrested in G2/M at the time of BrdU administration, and remained PH3+ throughout the 4-hour chase period. To test this possibility further, we allowed longer survival after BrdU administration (12 hours) to quantify loss of PH3 immunoreactivity in BrdU+ cells. Again, the percentage of BrdU+PH3+ cells was significantly higher in the Nestin:cKO SEZ and RMS (2.7±0.3 fold higher at P0, supplementary material Fig. S4; 3.6±1.0 fold higher at P21, Fig. 6A,B). Finally, to assess the proportion of progenitors within distinct stages of the cell cycle, SEZ and RMS cells were isolated from P0 and P21 animals, labeled with propidium iodide and subjected to flow cytometry. Normalization of flow data indicated significantly higher proportions of Nestin:cKO cells in G2/M compared with wild type at both P0 and P21 (Fig. 6C,D; supplementary material Fig. S4). These findings confirmed that NCSs and NPCs in Nestin:cKO brains were at least partially arrested in G2 and M phases of the cell cycle.

The defect in G2/M transition in *Sp2*-null brains prompted us to determine whether Nestin:cKO cells were capable of exiting the cell cycle at a similar rate to wild-type progenitors. To quantify cell cycle exiting, three pulses of BrdU were administered every 2 hours to P0 and P21 Nestin:cKO and cWT mice, followed by a 48-hour survival period (Fig. 6A,B; supplementary material Fig. S4). In this regimen, BrdU immunoreactivity was combined with Ki67 staining in order to distinguish progenitors that had remained in, or re-entered, the cell cycle after 48 hours (BrdU+/Ki67+), from cells that had exited the cell cycle (BrdU+/Ki67-negative). A significantly higher proportion of BrdU+ Nestin:cKO progenitors were Ki67+ compared with cWT progenitors, indicating a decline in cycle exiting (Fig. 6A,B). Thus, the extensive cell cycle analyses indicated that *Sp2*-null NSCs and NPCs were defective in G2-M transition, whereas S phase duration was relatively intact resulting

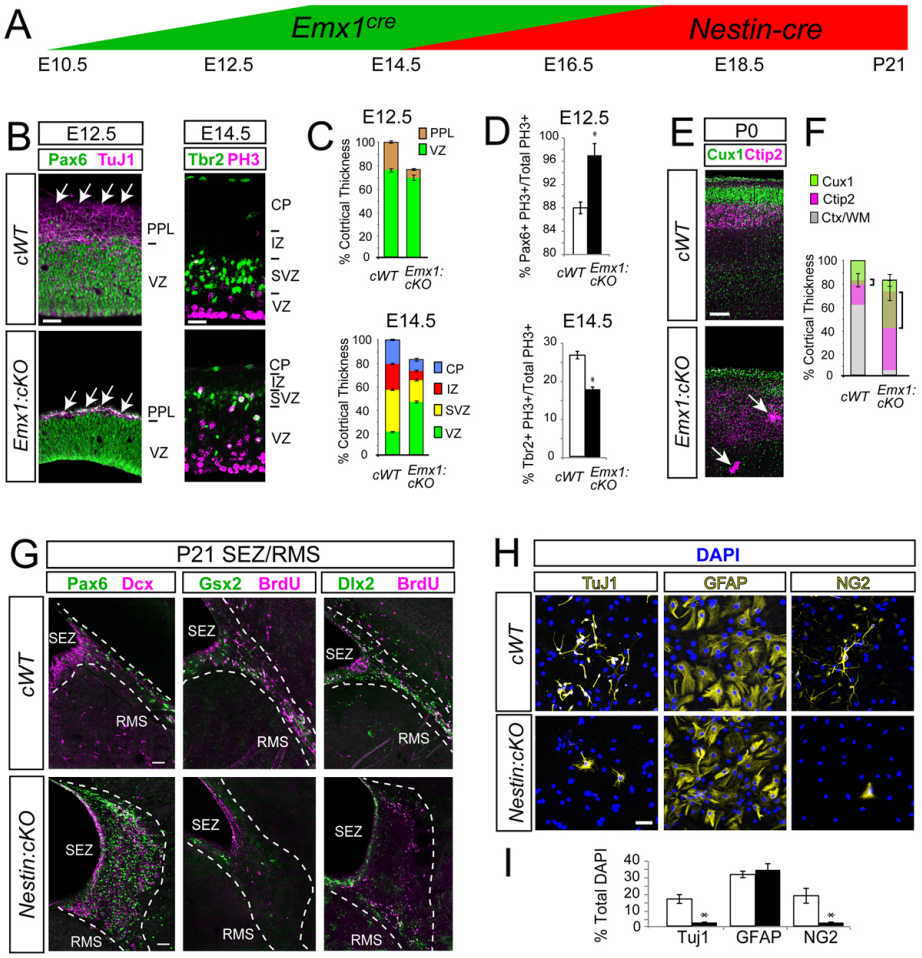

Fig. 7. Disruption of neurogenesis in the embryonic and postnatal *Sp2*-deleted brains. (**A**) Time graph illustrating the temporal efficiencies of the *Emx*^{cre} and *Nestin-cre* lines that were used to differentially delete *Sp2* in the embryonic and perinatal NSCs and NPCs (Liang et al., 2012). (B-F) Analyses of cWT and Emx1:cKO embryonic and P0 cerebral cortices. (**B**) Confocal micrographs of the embryonic cerebral cortex stained for Pax6 (green) and Tuj1 (purple) at E12.5 (arrows indicate the pial surface of the cortex), as well as Tbr2 (green) and PH3 (purple) at E14.5. (**C**) Percentage of total cortical thickness occupied by VZ and PPL at E12.5, and VZ, SVZ, IZ and CP at E14.5 (normalized to the average thickness of wild-type cortex). (**D**) Percentage of Pax6+ progenitors at E12.5, and Tbr2+ progenitors at E14.5, among all PH3+ cells in the wild-type and *Sp2* mutant cerebral cortices. (**E**) Confocal micrographs of Cux1 (green) and Ctip2 (purple) in the P0 cerebral cortex (arrows indicate ectopic clusters of Ctip2+ cells). (**F**) Percentage of total cortical and white matter thickness (gray) occupied by Cux1+ (green) and Ctip2+ (purple) projection neurons at P0 normalized to the average thickness of wild-type cortex. Brackets indicate degree of overlap between Cux1 and Ctip2 domains for each genotype. (G-I) Analysis of cWT and Nestin:cKO SEZ and RMS *in vivo* and *in vitro*. (**G**) Confocal micrographs of Pax6+ (green), Gsx2 (green) and Dlx2+ (green) NSCs and NPCs in the P21 SEZ and RMS (outlined by broken lines). Tissues were co-stained for Dcx and BrdU (1 hour acute pulse) as labeled (purple). (**H**) Confocal micrographs of cultured Tuj1+ neurons, GFAP+ astrocytes and NG2+ oligodendrocytes (yellow) obtained from cWT and Nestin:cKO SEZ and RMS progenitors, and differentiated for 6 days following neurosphere plating. (**I**) Percentages of each cell type among all DAPI-labeled nuclei (blue). Abbreviations: PPL, prelate; CP, cortical plate; IZ, intermediate zone; SVZ, subventricular zone; VZ, ventricular zone. Data are mean±s.e.m.; *P<0.05, Student's t-test, n=3/age group. Scale bars: 20 μm in B and G; 50 μm in E; 10 μm in H.

in a partial arrest in M. Interestingly, we also identified a significant reduction in the proportion of cells in G1/G0 (Fig. 6D), which may contribute towards a significant, yet moderate, increase in total cell cycle length in the cKO NSCs and NPCs in the postnatal brain (supplementary material Fig. S5).

Loss of Sp2 favors arrest of NSCs and NPCs in a Pax6 fate and severe disruption of neuronal and glial differentiation

We next sought to identify the impact of Sp2 deletion on the fate of NSC and NPC divisions. Differential timing of cre-mediated recombination in the *Emx1*^{cre} and *Nestin-cre* lines (Liang et al., 2012) was used to investigate effects on proliferative to neurogenic shifts during embryonic cortical development and on postnatal neurogenesis in the SEZ and RMS (Fig. 7A). To accomplish this, E12.5 Emx1:cKO and P21 Nestin:cKO brain sections were immunohistochemically labeled for various stage-specific progenitor markers and compared with cWT controls.

Nearly the entire thickness of the E12.5 Emx1:cKO cerebral cortex was occupied by Pax6+ cells, whereas cWT Pax6+ NSCs are confined to the VZ (Fig. 7B; supplementary material Fig. S6). Moreover, TuJ1+ postmitotic neurons were significantly reduced (Fig. 7B, arrows), resulting in a severe reduction in the size of the preplate (PPL; Fig. 7C). By E14.5, Tbr2+ NPCs were

significantly less dense in the Emx1:cKO SVZ (Fig. 7B; supplementary material Fig. S6), resulting in significant disruption in apico-basal organization of the cortex (Fig. 7C). Additionally, the percentage of PH3+/Pax6+ NSCs was significantly elevated at E12.5, whereas the percentage of PH3+ cells double labeled with Tbr2 was significantly reduced in the mutant basal VZ and SVZ at E14.5 (Fig. 7D); these defects could not be attributed to elevated apoptosis (supplementary material Fig. S7). Thus, it appeared that Pax6+ NSCs had expanded in the *Sp2*-null cerebral cortex at the expense of Tbr2+ NPCs and Tuj1+ neurons, suggesting defects in fate specification and differentiation in the early embryonic cortex.

To further examine the impact of Sp2 deletion on neuronal differentiation, laminar organization in the P0 Emx1:cKO cortex was assessed using Cux1 and Ctip2 immunostaining (Fig. 7E). In a mating scheme to generate Emx1:cKO P0 pups in 25% of pups in each litter, only 16% were obtained at birth (n=19; three independent litters), suggesting Emx1-mediated deletion of Sp2 was partially selected against *in utero*. In the few survivors, the thickness of the cortex was compromised (Fig. 7F): Cux1+ cells were largely absent in the upper cortical layers and distribution of Ctip2+ cells failed to specify layer V in the way that they did in cWT cortices (Fig. 7E,F). Additionally, ectopic and densely packed clusters of Ctip2+ cells were detected in the P0 cortex, suggesting disruption of their differentiation or migration (Fig. 7E, arrows).

To determine whether perinatal deletion of Sp2 would similarly impact lineal relationships between postnatal NSCs and NPCs, we used Pax6, Dlx2 and Gsx2 staining in the Nestin:cKO SEZ and RMS. Remarkably, *Sp2* deletion resulted in accumulation of Pax6+ cells concomitant with disruption of Gsx2+ or Dlx2+ progenitors and Dcx2+ neuroblasts in the mutant SEZ and RMS (Fig. 7G). In contrast to the embryonic period, a clear increase in the number of apoptotic cells was noted in the Nestin:cKO SEZ/RMS 'bulge' area at P21 (supplementary material Fig. S7). As apoptotic cells emerged only during postnatal stages, they most likely represent secondary defects rather than a direct consequence of Sp2 deletion.

Finally, to assess the impact of Sp2 on the differentiation potential of postnatal NSCs and NPCs, P21 Nestin:cKO SEZ and RMS cells were cultured to generate neurospheres followed by plating for differentiation (Fig. 7H). Although cWT neurospheres generated astrocytes (GFAP+), oligodendrocytes (NG2+) and neurons (Tuj1+), cKO neurospheres were largely astrocytogenic, and their ability to differentiate into oligodendrocytes or neurons was significantly impaired (Fig. 7H). Thus, these results suggest that Sp2-dependent regulation of the cell cycle is required to drive the progeny of cycling NSCs and NPCs towards their programmed neuronal and glial fates during corticogenesis and postnatal neurogenesis. Disruption of Sp2-dependent cell cycle progression appears to favor the maintenance of an early NSC type in the developing and postnatal stem cell niches.

DISCUSSION

Sp2 is a novel regulator of cell cycle progression

The present study uncovered a novel role for the transcription factor Sp2 in cell cycle homeostasis within developing NSCs and NPCs. A combination of approaches in this study led to identification of M-phase arrest, rapid G2/M transition and shorter G1, whereas the S phase appears intact in *Sp2*-null NSCs and NPCs. This function of Sp2 is not confined to a specific developmental stage, but equally impacts embryonic and postnatal NSCs and NPCs. M-phase arrest in embryonic and postnatal *Sp2*-null NSCs and NPCs is concomitant with overall decline in the number of cycling cells, which is consistent with the notion that proper progression through mitosis is required for maintenance of neural progenitor pools during brain development (Feng and Walsh, 2004; Silver et al., 2008; Lizarraga et al., 2010; Gruber et al., 2011; Sakai et al., 2012; Lian et al., 2012). However, unlike the mitotic arrest due to deletion of Tcof1/Treakle (a centrosomal protein), which results in reduction of both apical and basal cortical progenitors (Sakai et al., 2012), our findings show that Sp2-dependent mitotic arrest may preferentially expand apical NSCs at the expense of basal NPCs. As several M-phase regulators such as Aurora-A and Polo kinase can exert dual roles in cell cycle progression and fate determination (reviewed by Budirahardja and Gönczy, 2009), it is conceivable that potential crosstalk between Sp2 functions and various cell cycle-active kinases may couple M progression with fate specification in NSCs and NPCs. Such coupling may differentially impact symmetric and asymmetric cell divisions in apical and basal progenitors of the cerebral cortex.

In addition to M-phase arrest in NSCs and NPCs, transition through G2 is accelerated in the absence of Sp2. In this context, the mitotic entry network involves upregulation of the cyclin B1-Cdk1 complex and its activation through post-transcriptional modifications (Fung and Poon, 2005; White et al., 2009; Lindqvist et al., 2009; Bollen et al., 2009). Notably, many kinases and phosphatases that form the mitotic entry network are also required for progression through M (Pomerening et al., 2008; Lindqvist et al., 2009; Bollen et al., 2009), for example by coupling timely G2-M transition to centrosome maturation for appropriate mitotic spindle orientation in neural progenitors (Gruber et al., 2011). At this juncture, it remains unclear how Sp2-dependent mechanisms regulate G2-M transition in parallel with M-phase progression.

Our long-term BrdU-tracing experiments revealed a lower rate of cell cycle exiting in *Sp2* mutant progenitors, which can be explained by arrest in M or by cell cycle re-entry instead of cell cycle exit. However, *Sp2*-null progenitors exhibit only a moderate increase in total cell cycle length, which may, at least in part, be due to a simultaneous decline in G1 duration (indicated by flow data) combined with a prolonged M. Thus, it appears that *Sp2*-null progenitors have shortened gap phases, a prolonged M phase and probably re-enter the cell cycle constitutively, which is likely to be the cause of the rapid decline in total NSCs and NPCs due to precocious senescence and absence of mechanisms for quiescence. In this situation, an intriguing parallel may be drawn regarding the lack of, or very brief, G1 and G2 in early embryonic stem cells (Burdon et al., 2002; Stead et al., 2002). As development proceeds, the two gap phases emerge and progressively lengthen (especially G1) with a concomitant decline in the rate of stem cell divisions (He et al., 2009). By the time the neuroepithelium is specified, the two gap phases are established in early NSCs; however, the length of G1 is significantly shorter in cerebral cortical progenitors at early (E11.5 in the mouse) versus late (E16.5 in the mouse) stages of development (Takahashi et al., 1996). Gap phase alterations are crucial for prolonged maintenance of NSCs and NPCs, as well as influencing the fate of their neuronal and glial progenies (Smith and Luskin, 1998; Cameron and McKay, 2001; Hayes and Nowakowski, 2002; Burns and Kuan, 2005; Lu et al., 2007). The perturbed duration of gap phases in *Sp2*-null NSCs and NPCs at least partially resembles early stem cells, which suggests that Sp2-dependent mechanisms may be important regulators of cell cycle maturation in stem cells and progenitors during embryonic and postnatal development.

Sp2 deletion impacts the fate of NSC and NPC progenies

Numerous studies have illustrated changes in cell cycle compartments that impact neurogenesis and the differentiation potential of NSCs and NPCs. For example, the total length of the cell cycle and the duration of G1 clearly impact neurogenic NPCs compared with early proliferative NSCs (Calegari et al., 2005; Salomoni and Calegari, 2010). Furthermore, lengthening of G1 is highly correlated with the transition from apical NSCs to basal NPCs in the developing cortex (Arai et al., 2011). Similarly, lengthening the cell cycle promotes expansion of the NPC pool and enhances neuronal production in human neural progenitors (García-García et al., 2012). Moreover, as G2 lengthens during embryonic development it slows the rate of S-G2-M transition in basal NPCs, but not in apical NSCs (Calegari et al., 2005). Thus, the normal maintenance of a stem cell niche entails preservation of some progenitors with characteristics of developmentally early NSCs, as is also evident in the presence of slow-dividing NSCs in the adult mouse SEZ (Doetsch et al., 1999a; Doetsch et al., 1999b).

Disruption of the cell cycle in the absence of Sp2 severely impacts fate specification in NSCs and NPCs, where a significant expansion of Pax6+ NSCs is in conjunction with depletion of Tbr2+ NPCs, and correlates with near absence of postmitotic neurons in the cortical plate, a lineage that is well established (Englund et al., 2005; Sessa et al., 2008). A conceptually similar phenotype was apparent in the SEZ/RMS of *Nestin-cre*-deleted *Sp2* brains where presumptive Pax6+ NSCs were expanded, whereas the Gsx2+ and Dlx2+ NSCs and NPCs were relatively unaffected in the mutant SEZ. This observation is in sync with a past report that Pax6 deletion leads to ectopic upregulation of Dlx2 in the dorsal telencephalon (Toresson et al., 2000). However, these findings must be interpreted cautiously as the lineal relationships among Pax6-, Gsx2- and Dlx2-expressing populations in the postnatal SEZ and RMS are complex, partially overlapping and likely to be nonlinear (Brill et al., 2008). Whether the misregulated timing of NPC expansion as well as neuronal production directly contribute to the defects in the cortical progenitor organization still remains to be determined. In addition, Sp2-dependent cell cycle regulation appears to be required for differentiation of both postnatal neuronal and oligodendroglial lineages by functioning as a key regulator of the switch from proliferation to differentiation in NSCs and NPCs. How the timing of cell cycle progression regulates programmed fate decisions during neurogenesis and gliogenesis remains largely unknown.

Implications and conclusions

In summary, our study reveals for the first time that Sp2-dependent regulation of transitions through distinct cell cycle phases is crucial for developmental maturation of early embryonic NSCs into neurogenic and gliogenic NPCs in the cortex and the postnatal stem cell niche. How Sp2 carries out these important functions is the subject of future studies. The molecular mechanisms underlying the role of Sp2 as a putative transcription factor have remained largely enigmatic; while a recent study implicates Sp2 as a global transcriptional regulator (Terrados et al., 2012), a number of past studies failed to identify strong DNA-binding or transcriptional activity by Sp2, suggesting these functions of Sp2 may be negatively regulated in mammalian cells (e.g. Moorefield et al., 2004). At this juncture, it is tempting to speculate that loss of Sp2 may severely impact symmetric and asymmetric decisions in NSCs and NPCs through misregulation of cell cycle progression and in particular G2/M progression. An important future direction of the current work is to determine whether or not Sp2 directly participates in symmetric and asymmetric division of NSCs and NPCs in the developing and postnatal brains as a putative transcription factor or through alternative cell biological roles. Conditional deletion of *Sp2* will provide a suitable model for studying the link between cell cycle regulation and fate specification in NSCs and NPCs in these future studies.

Acknowledgements:
We thank Drs. E. Tucker and A. Barnes for discussions and critical reading of the manuscript and Dr L. Luo for the MADM-11 mice.

Funding
This work was supported by a National Institutes of Health grant [R01NS062182], by a grant from the American Federation for Aging Research and by generous institutional funds to H.T.G. Deposited in PMC for release after 12 months.

Competing interests statement
The authors declare no competing financial interests.

Supplementary material
Supplementary material available online at
http://dev.biologists.org/lookup/suppl/doi:10.1242/dev.085621/-/DC1

References

Arai, Y., Pulvers, J. N., Haffner, C., Schilling, B., Nüsslein, I., Calegari, F. and Huttner, W. B. (2011). Neural stem and progenitor cells shorten S-phase on commitment to neuron production. *Nat Commun.* **2**, 154.
Baur, F., Nau, K., Sadic, D., Allweiss, L., Elsässer, H. P., Gillemans, N., de Wit, T., Krüger, I., Vollmer, M., Philipsen, S. et al. (2010). Specificity protein 2 (Sp2) is essential for mouse development and autonomous proliferation of mouse embryonic fibroblasts. *PLoS ONE* **5**, e9587.
Black, A. R., Black, J. D. and Azizkhan-Clifford, J. (2001). Sp1 and krüppel-like factor family of transcription factors in cell growth regulation and cancer. *J. Cell. Physiol.* **188**, 143-160.
Bollen, M., Gerlich, D. W. and Lesage, B. (2009). Mitotic phosphatases: from entry guards to exit guides. *Trends Cell Biol.* **19**, 531-541.
Bouwman, P., Göllner, H., Elsässer, H. P., Eckhoff, G., Karis, A., Grosveld, F., Philipsen, S. and Suske, G. (2000). Transcription factor Sp3 is essential for post-natal survival and late tooth development. *EMBO J.* **19**, 655-661.
Brill, M. S., Snapyan, M., Wohlfrom, H., Ninkovic, J., Jawerka, M., Mastick, G. S., Ashery-Padan, R., Saghatelyan, A., Berninger, B. and Götz, M. (2008). A dlx2- and pax6-dependent transcriptional code for periglomerular neuron specification in the adult olfactory bulb. *J. Neurosci.* **28**, 6439-6452.
Budirahardja, Y. and Gönczy, P. (2009). Coupling the cell cycle to development. *Development* **136**, 2861-2872.
Burdon, T., Smith, A. and Savatier, P. (2002). Signalling, cell cycle and pluripotency in embryonic stem cells. *Trends Cell Biol.* **12**, 432-438.
Burns, K. A. and Kuan, C. Y. (2005). Low doses of bromo- and iododeoxyuridine produce near-saturation labeling of adult proliferative populations in the dentate gyrus. *Eur. J. Neurosci.* **21**, 803-807.
Calegari, F., Haubensak, W., Haffner, C. and Huttner, W. B. (2005). Selective lengthening of the cell cycle in the neurogenic subpopulation of neural progenitor cells during mouse brain development. *J. Neurosci.* **25**, 6533-6538.
Cameron, H. A. and McKay, R. D. (2001). Adult neurogenesis produces a large pool of new granule cells in the dentate gyrus. *J. Comp. Neurol.* **435**, 406-417.
Costa, M. R., Götz, M. and Berninger, B. (2010). What determines neurogenic competence in glia? *Brain Res. Rev.* **63**, 47-59.
Doetsch, F., Caillé, I., Lim, D. A., García-Verdugo, J. M. and Alvarez-Buylla, A. (1999a). Subventricular zone astrocytes are neural stem cells in the adult mammalian brain. *Cell* **97**, 703-716.
Doetsch, F., García-Verdugo, J. M. and Alvarez-Buylla, A. (1999b). Regeneration of a germinal layer in the adult mammalian brain. *Proc. Natl. Acad. Sci. USA* **96**, 11619-11624.
Englund, C., Fink, A., Lau, C., Pham, D., Daza, R. A., Bulfone, A., Kowalczyk, T. and Hevner, R. F. (2005). Pax6, Tbr2, and Tbr1 are expressed sequentially by radial glia, intermediate progenitor cells, and postmitotic neurons in developing neocortex. *J. Neurosci.* **25**, 247-251.
Farkas, L. M. and Huttner, W. B. (2008). The cell biology of neural stem and progenitor cells and its significance for their proliferation versus differentiation during mammalian brain development. *Curr. Opin. Cell Biol.* **20**, 707-715.
Feng, Y. and Walsh, C. A. (2004). Mitotic spindle regulation by Nde1 controls cerebral cortical size. *Neuron* **44**, 279-293.

Fietz, S. A. and Huttner, W. B. (2011). Cortical progenitor expansion, self-renewal and neurogenesis-a polarized perspective. *Curr. Opin. Neurobiol.* **21**, 23-35.
Fung, T. K. and Poon, R. Y. (2005). A roller coaster ride with the mitotic cyclins. *Semin. Cell Dev. Biol.* **16**, 335-342.
García-García, E., Pino-Barrio, M. J., López-Medina, L. and Martínez-Serrano, A. (2012). Intermediate progenitors are increased by lengthening of the cell cycle through calcium signaling and p53 expression in human neural progenitors. *Mol. Biol. Cell* **23**, 1167-1180.
Göllner, H., Bouwman, P., Mangold, M., Karis, A., Braun, H., Rohner, I., Del Rey, A., Besedovsky, H. O., Meinhardt, A., van den Broek, M. et al. (2001). Complex phenotype of mice homozygous for a null mutation in the Sp4 transcription factor gene. *Genes Cells* **6**, 689-697.
Götz, M. and Huttner, W. B. (2005). The cell biology of neurogenesis. *Nat. Rev. Mol. Cell Biol.* **6**, 777-788.
Gruber, R., Zhou, Z., Sukchev, M., Joerss, T., Frappart, P. O. and Wang, Z. Q. (2011). MCPH1 regulates the neuroprogenitor division mode by coupling the centrosomal cycle with mitotic entry through the Chk1-Cdc25 pathway. *Nat. Cell Biol.* **13**, 1325-1334.
Guillemot, F. (2007). Cell fate specification in the mammalian telencephalon. *Prog. Neurobiol.* **83**, 37-52.
Hand, R., Bortone, D., Mattar, P., Nguyen, L., Heng, J. I., Guerrier, S., Boutt, E., Peters, E., Barnes, A. P., Parras, C. et al. (2005). Phosphorylation of Neurogenin2 specifies the migration properties and the dendritic morphology of pyramidal neurons in the neocortex. *Neuron* **48**, 45-62.
Haubensak, W., Attardo, A., Denk, W. and Huttner, W. B. (2004). Neurons arise in the basal neuroepithelium of the early mammalian telencephalon: a major site of neurogenesis. *Proc. Natl. Acad. Sci. USA* **101**, 3196-3201.
Hayes, N. L. and Nowakowski, R. S. (2002). Dynamics of cell proliferation in the adult dentate gyrus of two inbred strains of mice. *Brain Res. Dev. Brain Res.* **134**, 77-85.
He, S., Nakada, D. and Morrison, S. J. (2009). Mechanisms of stem cell self-renewal. *Annu. Rev. Cell Dev. Biol.* **25**, 377-406.
Hippenmeyer, S., Youn, Y. H., Moon, H. M., Miyamichi, K., Zong, H., Wynshaw-Boris, A. and Luo, L. (2010). Genetic mosaic dissection of Lis1 and Ndel1 in neuronal migration. *Neuron* **68**, 695-709.
Jacquet, B. V., Patel, M., Iyengar, M., Liang, H., Therit, B., Salinas-Mondragon, R., Lai, C., Olsen, J. C., Anton, E. S. and Ghashghaei, H. T. (2009a). Analysis of neuronal proliferation, migration and differentiation in the postnatal brain using equine infectious anemia virus-based lentiviral vectors. *Gene Ther.* **16**, 1021-1033.
Jacquet, B. V., Salinas-Mondragon, R., Liang, H., Therit, B., Buie, J. D., Dykstra, M., Campbell, K., Ostrowski, L. E., Brody, S. L. and Ghashghaei, H. T. (2009b). FoxJ1-dependent gene expression is required for differentiation of radial glia into ependymal cells and a subset of astrocytes in the postnatal brain. *Development* **136**, 4021-4031.
Jacquet, B. V., Ruckart, P. and Ghashghaei, H. T. (2010). An organotypic slice assay for high-resolution time-lapse imaging of neuronal migration in the postnatal brain. *J. Vis. Exp.* **11**, 2486.
Kim, T. H., Chiera, S. L., Linder, K. E., Trempus, C. S., Smart, R. C. and Horowitz, J. M. (2010). Overexpression of transcription factor sp2 inhibits epidermal differentiation and increases susceptibility to wound- and carcinogen-induced tumorigenesis. *Cancer Res.* **70**, 8507-8516.
Kriegstein, A. and Alvarez-Buylla, A. (2009). The glial nature of embryonic and adult neural stem cells. *Annu. Rev. Neurosci.* **32**, 149-184.
Krüger, I., Vollmer, M., Simmons, D. G., Elsässer, H. P., Philipsen, S. and Suske, G. (2007). Sp1/Sp3 compound heterozygous mice are not viable: impaired erythropoiesis and severe placental defects. *Dev. Dyn.* **236**, 2235-2244.
Lian, G., Lu, J., Hu, J., Zhang, J., Cross, S. H., Ferland, R. J. and Sheen, V. L. (2012). Filamin a regulates neural progenitor proliferation and cortical size through Wee1-dependent Cdk1 phosphorylation. *J. Neurosci.* **32**, 7672-7684.
Liang, H., Hippenmeyer, S. and Ghashghaei, H. T. (2012). A *Nestin-cre* transgenic mouse is insufficient for recombination in early embryonic neural progenitors. *Biol. Open* **1**, 1200-1203.
Lindqvist, A., Rodríguez-Bravo, V. and Medema, R. H. (2009). The decision to enter mitosis: feedback and redundancy in the mitotic entry network. *J. Cell Biol.* **185**, 193-202.
Lizarraga, S. B., Margossian, S. P., Harris, M. H., Campagna, D. R., Han, A. P., Blevins, S., Mudbhary, R., Barker, J. E., Walsh, C. A. and Fleming, M. D. (2010). Cdk5rap2 regulates centrosome function and chromosome segregation in neuronal progenitors. *Development* **137**, 1907-1917.
Lu, M., Zhang, R. L., Zhang, Z. G., Yang, J. J. and Chopp, M. (2007). Linkage of cell cycle kinetics between embryonic and adult stroke models: an analytical approach. *J. Neurosci. Methods* **161**, 323-330.
Manzini, M. C. and Walsh, C. A. (2011). What disorders of cortical development tell us about the cortex: one plus one does not always make two. *Curr. Opin. Genet. Dev.* **21**, 333-339.
Marin, M., Karis, A., Visser, P., Grosveld, F. and Philipsen, S. (1997). Transcription factor Sp1 is essential for early embryonic development but dispensable for cell growth and differentiation. *Cell* **89**, 619-628.
Martynoga, B., Morrison, H., Price, D. J. and Mason, J. O. (2005). Foxg1 is required for specification of ventral telencephalon and region-specific regulation of dorsal telencephalic precursor proliferation and apoptosis. *Dev. Biol.* **283**, 113-127.
Miyata, T., Kawaguchi, A., Saito, K., Kawano, M., Muto, T. and Ogawa, M. (2004). Asymmetric production of surface-dividing and non-surface-dividing cortical progenitor cells. *Development* **131**, 3133-3145.
Moorefield, K. S., Fry, S. J. and Horowitz, J. M. (2004). Sp2 DNA binding activity and trans-activation are negatively regulated in mammalian cells. *J. Biol. Chem.* **279**, 13911-13924.
Nguyên-Trân, V. T., Kubalak, S. W., Minamisawa, S., Fiset, C., Wollert, K. C., Brown, A. B., Ruiz-Lozano, P., Barrere-Lemaire, S., Kondo, R., Norman, L. W. et al. (2000). A novel genetic pathway for sudden cardiac death via defects in the transition between ventricular and conduction system cell lineages. *Cell* **102**, 671-682.
Noctor, S. C., Martínez-Cerdeño, V., Ivic, L. and Kriegstein, A. R. (2004). Cortical neurons arise in symmetric and asymmetric division zones and migrate through specific phases. *Nat. Neurosci.* **7**, 136-144.
Okano, H. and Temple, S. (2009). Cell types to order: temporal specification of CNS stem cells. *Curr. Opin. Neurobiol.* **19**, 112-119.
Pinto, L. and Götz, M. (2007). Radial glial cell heterogeneity – the source of diverse progeny in the CNS. *Prog. Neurobiol.* **83**, 2-23.
Pomerening, J. R., Ubersax, J. A. and Ferrell, J. E., Jr (2008). Rapid cycling and precocious termination of G1 phase in cells expressing CDK1AF. *Mol. Biol. Cell* **19**, 3426-3441.
Pontious, A., Kowalczyk, T., Englund, C. and Hevner, R. F. (2008). Role of intermediate progenitor cells in cerebral cortex development. *Dev. Neurosci.* **30**, 24-32.
Reynolds, B. A. and Weiss, S. (1992). Generation of neurons and astrocytes from isolated cells of the adult mammalian central nervous system. *Science* **255**, 1707-1710.
Sakai, D., Dixon, J., Dixon, M. J. and Trainor, P. A. (2012). Mammalian neurogenesis requires Treacle-Plk1 for precise control of spindle orientation, mitotic progression, and maintenance of neural progenitor cells. *PLoS Genet.* **8**, e1002566.
Salomoni, P. and Calegari, F. (2010). Cell cycle control of mammalian neural stem cells: putting a speed limit on G1. *Trends Cell Biol.* **20**, 233-243.
Sessa, A., Mao, C. A., Hadjantonakis, A. K., Klein, W. H. and Broccoli, V. (2008). Tbr2 directs conversion of radial glia into basal precursors and guides neuronal amplification by indirect neurogenesis in the developing neocortex. *Neuron* **60**, 56-69.
Silver, D. L., Hou, L., Somerville, R., Young, M. E., Apte, S. S. and Pavan, W. J. (2008). The secreted metalloprotease ADAMTS20 is required for melanoblast survival. *PLoS Genet.* **4**, e1000003.
Singh, A. M. and Dalton, S. (2009). The cell cycle and Myc intersect with mechanisms that regulate pluripotency and reprogramming. *Cell Stem Cell* **5**, 141-149.
Smith, C. M. and Luskin, M. B. (1998). Cell cycle length of olfactory bulb neuronal progenitors in the rostral migratory stream. *Dev. Dyn.* **213**, 220-227.
Stead, E., White, J., Faast, R., Conn, S., Goldstone, S., Rathjen, J., Dhingra, U., Rathjen, P., Walker, D. and Dalton, S. (2002). Pluripotent cell division cycles are driven by ectopic Cdk2, cyclin A/E and E2F activities. *Oncogene* **21**, 8320-8333.
Supp, D. M., Witte, D. P., Branford, W. W., Smith, E. P. and Potter, S. S. (1996). Sp4, a member of the Sp1-family of zinc finger transcription factors, is required for normal murine growth, viability, and male fertility. *Dev. Biol.* **176**, 284-299.
Takahashi, T., Nowakowski, R. S. and Caviness, V. S., Jr (1996). The leaving or Q fraction of the murine cerebral proliferative epithelium: a general model of neocortical neuronogenesis. *J. Neurosci.* **16**, 6183-6196.
Terrados, G., Finkernagel, F., Stielow, B., Sadic, D., Neubert, J., Herdt, O., Krause, M., Scharfe, M., Jarek, M. and Suske, G. (2012). Genome-wide localization and expression profiling establish Sp2 as a sequence-specific transcription factor regulating vitally important genes. *Nucleic Acids Res.* **40**, 7844-7857.
Toresson, H., Potter, S. S. and Campbell, K. (2000). Genetic control of dorsal-ventral identity in the telencephalon: opposing roles for Pax6 and Gsh2. *Development* **127**, 4361-4371.
van Loo, P. F., Bouwman, P., Ling, K. W., Middendorp, S., Suske, G., Grosveld, F., Dzierzak, E., Philipsen, S. and Hendriks, R. W. (2003). Impaired hematopoiesis in mice lacking the transcription factor Sp3. *Blood* **102**, 858-866.
White, M. A., Riles, L. and Cohen, B. A. (2009). A systematic screen for transcriptional regulators of the yeast cell cycle. *Genetics* **181**, 435-446.
Xie, J., Yin, H., Nichols, T. D., Yoder, J. A. and Horowitz, J. M. (2010). Sp2 is a maternally inherited transcription factor required for embryonic development. *J. Biol. Chem.* **285**, 4153-4164.
Yin, H., Nichols, T. D. and Horowitz, J. M. (2010). Transcription of mouse Sp2 yields alternatively spliced and sub-genomic mRNAs in a tissue- and cell-type-specific fashion. *Biochim. Biophys. Acta* **1799**, 520-531.

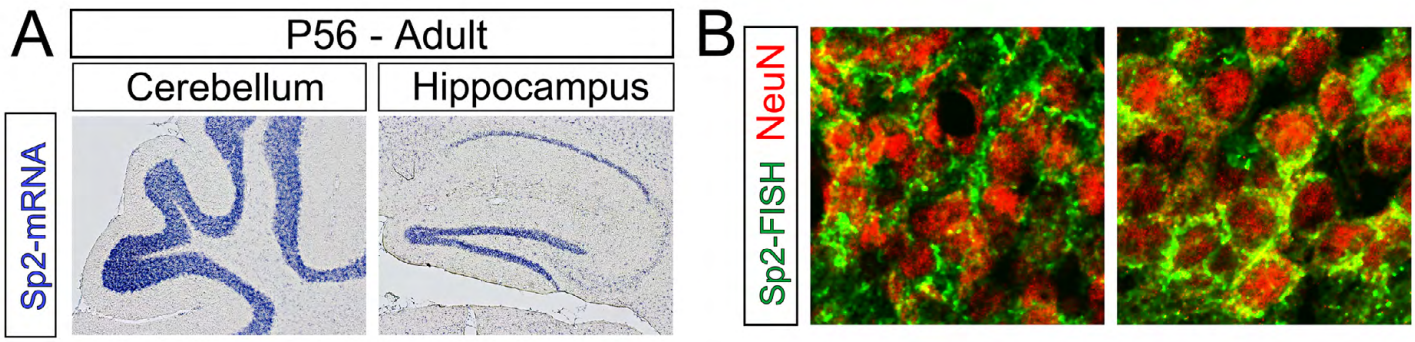

Fig. S1. Sp2 expression in the cerebellum and hippocampus of a P56 adult mouse. (**A**) *Sp2* is expressed in granular layers of the cerebellum and hippocampus in sagittal sections processed to visualize a DIG-labeled *Sp2* probe (blue). (**B**) Fluorescence in situ hybridization against the *Sp2* probe (green) co-labeled with NeuN (red) in corresponding granular layer of the cerebellum and the dentate gyrus of the hippocampus.

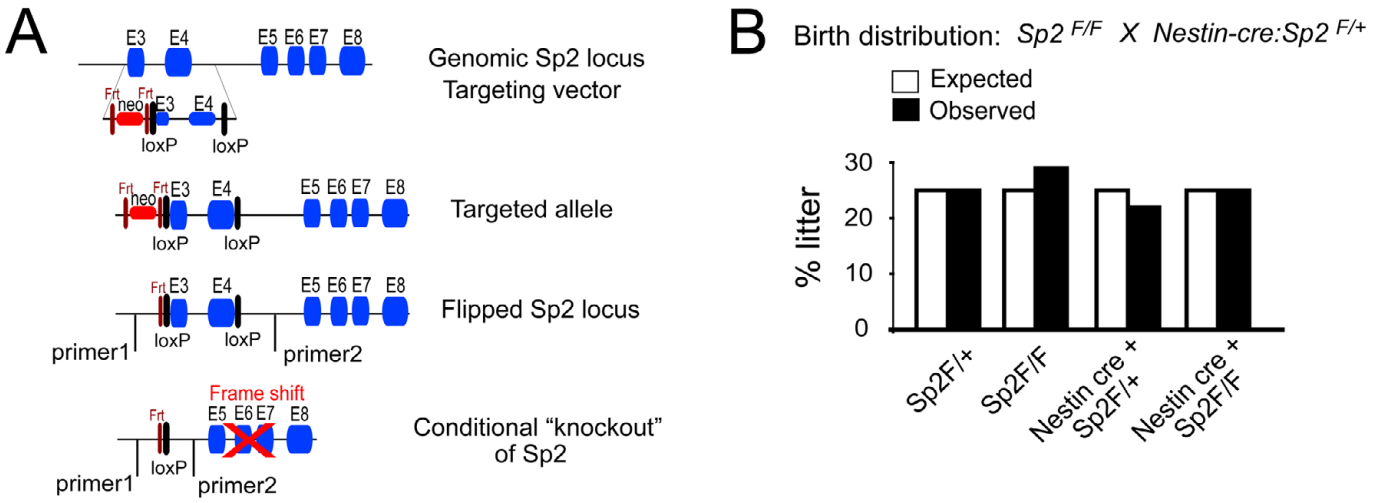

Fig. S2. Generation and analysis of the *Sp2* floxed mice. (**A**) A targeting vector containing an HSVtk-neo cassette (red bar) upstream of *Sp2* exon 3 was generated. LoxP sites (black boxes) were introduced to flank *Sp2* exon 3 and exon 4. Frt sites on both sides of the neo cassette allowed for its removal in targeted ES cells using flip-mediated recombination. Mice carrying the *Sp2* 'floxed' locus were interbred with *Nestin-cre* transgenic mice, which resulted in deletion of exons 3 and 4 in tissue harvested from the postnatal brain. (**B**) Birth rate of offspring from [*Sp2* $^{F/F}$] crossed to [*Nestin-cre(het):Sp2*$^{F/+}$] mice. The expected genotypes based on Mendelian ratios are 25% for genotypes [Sp2$^{F/+}$], [Sp2 $^{F/F}$], [*Nestin-cre(het):Sp2*$^{F/+}$] and [*Nestin-cre(het):Sp2*$^{F/F}$]. Percentages were calculated for the total number of mice (*n*=203, from 22 litters).

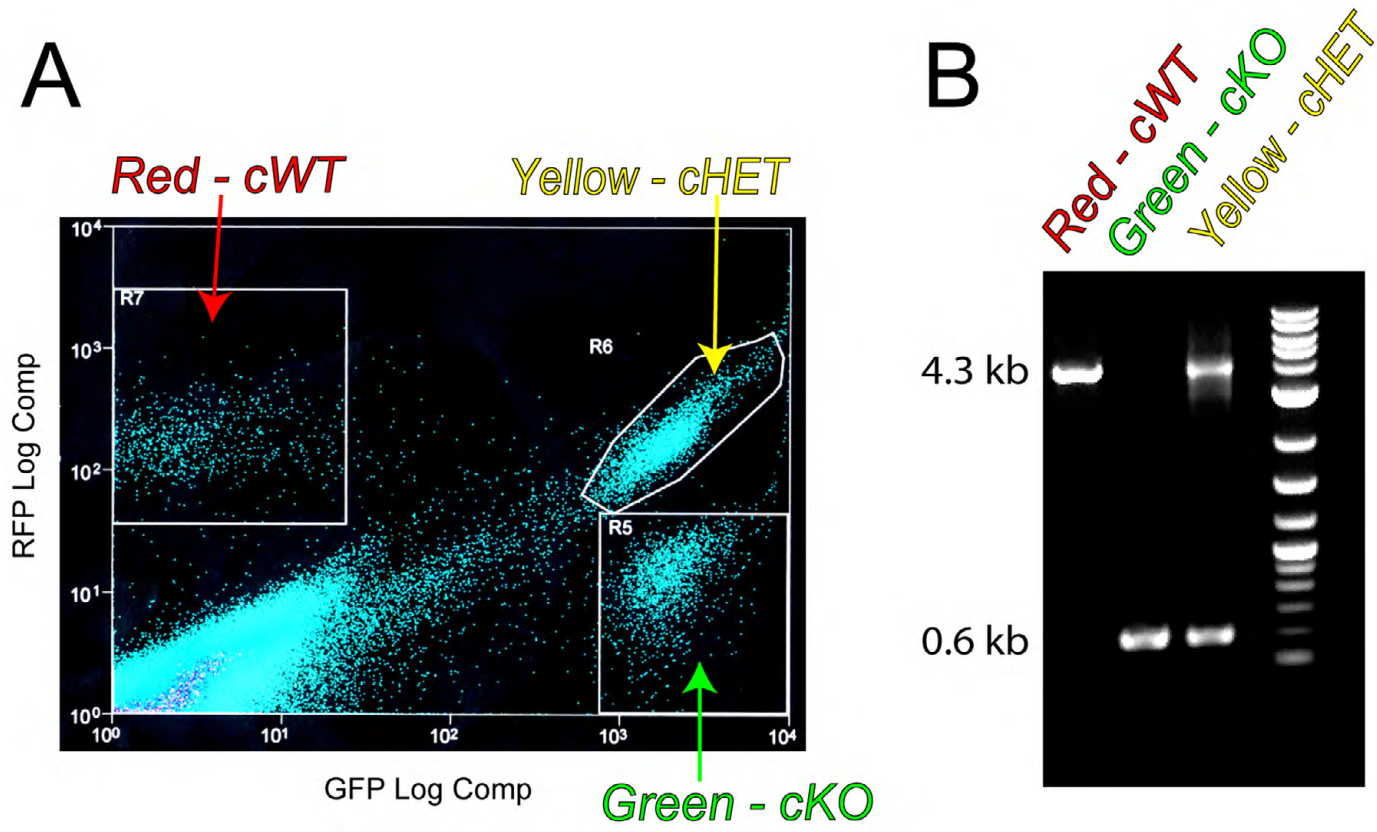

Fig. S3. Distinctly labeled MADM-11 cells faithfully carry allelic deletion of *Sp2* corresponding to expected combinatorial expression of fluorophores. (**A**) *Nestin-cre:Sp2* $^{F/+}$*:MADM-11* cells from P0 mice were harvested and isolated using fluorescence activated cell sorting. (**B**) PCR analysis of DNA confirmed genotypes of distinctly sorted populations corresponding to red=cWT, green=cKO and yellow=cHet genotypes.

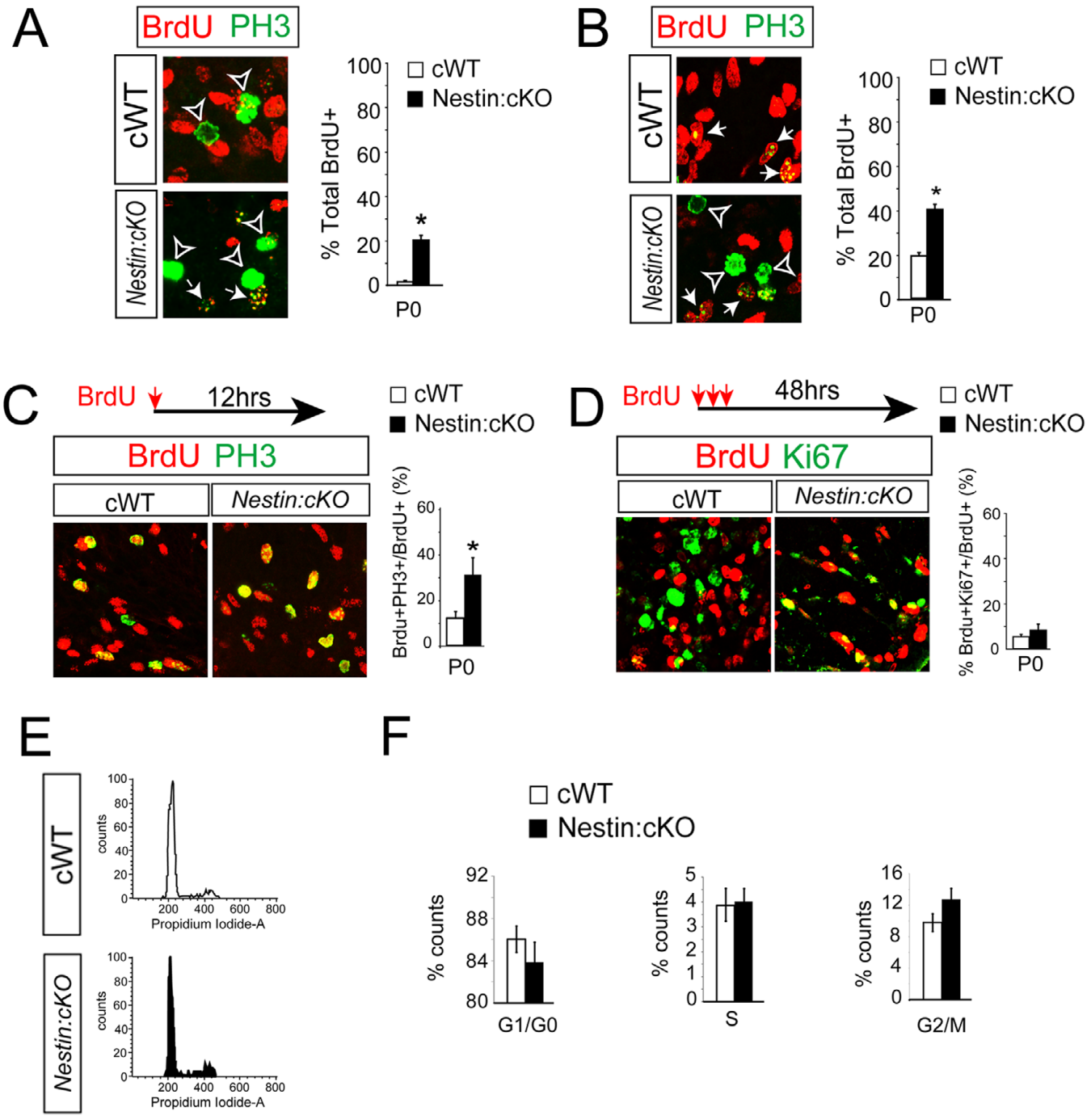

Fig. S4. Cell cycle progression from S-to-G2/M is disrupted in Nestin:cKO progenitors harvested at P0. (**A**) A 1-hour BrdU pulse-chase experiments allowed for identification of proliferating cells that progressed from S to G2/M phases of the cell cycle by co-labeling BrdU (red) with the M-phase marker PH3 (green; arrows). M-phase cells that did not incorporate BrdU during the 1-hour chase period were labeled as PH3+/BrdU negative (arrow heads). The proportion of BrdU+ cells in the SEZ and RMS of Nestin:cKO mice that progressed into G2/M (PH3+) was consistently and significantly higher compared with cWT progenitors at P0. (**B**) Four-hour BrdU pulse-chase experiments allowed for identification of proliferating Nestin:cKO progenitors that exhibit M phase perdurance. Arrows indicate BrdU+/PH3+ cells; arrowheads indicate BrdU-negative/PH3+ cells. Percentage of BrdU+/PH3+ cells among all BrdU incorporated cells is significantly increased in P0 mutant compared with the control. In addition, a significant fraction of PH3+ cells in the Nestin:cKO SEZ and RMS remained BrdU negative. (**C**) BrdU administration followed by 12 hours of chase allowed for indexing M-phase exiting. The percentage of BrdU+/PH3+ cells in the Nestin:cKO SEZ and RMS was significantly higher than in cWT brains. (**D**) To quantify cell cycle exiting, three pulses of BrdU were administered every 2 hours followed by a 48-hour survival period. In this regimen, BrdU immunoreactivity was combined with Ki67 staining in order to distinguish progenitors that had remained in, or re-entered, the cell cycle after 48 hours (BrdU+/Ki67+) from cells that had exited the cell cycle (BrdU+/Ki67 negative). Percentage of BrdU+/Ki67+ cells among all BrdU incorporated cells is higher in the Nestin:cKO SEZ/RMS compared with controls. For A-D, data are mean±s.e.m.; *P<0.05, Student's t-test, n=3/age group. (**E**,**F**) Flow cytometry for cell cycle analysis at P0. Data from cycling cells harvested from P0 SEZ and RMS illustrated higher proportion of cells in the G2/M phases in Nestin:cKOs. *P<0.01, Student's t-test, n=3/age group.

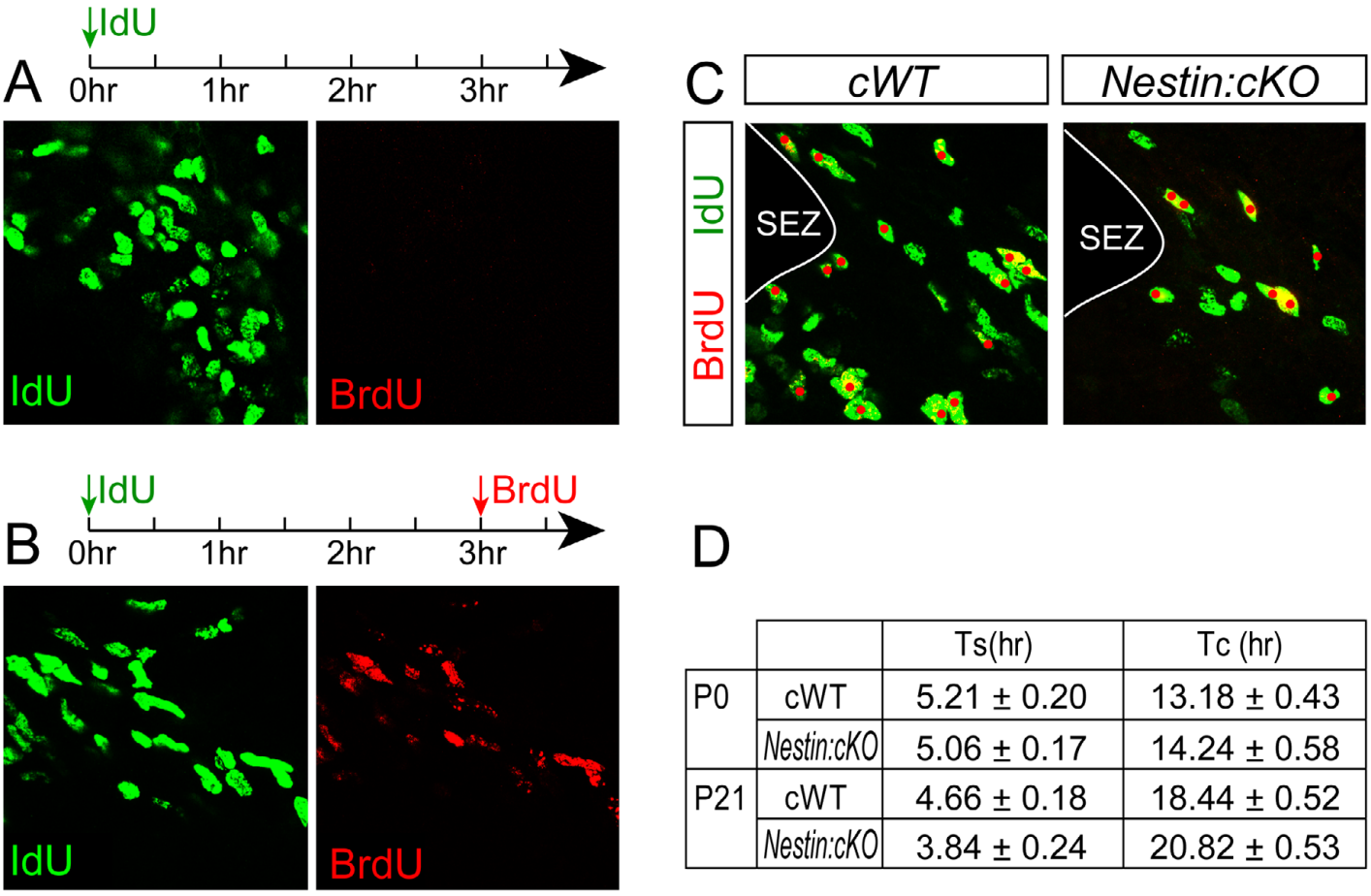

		Ts(hr)	Tc (hr)
P0	cWT	5.21 ± 0.20	13.18 ± 0.43
	Nestin:cKO	5.06 ± 0.17	14.24 ± 0.58
P21	cWT	4.66 ± 0.18	18.44 ± 0.52
	Nestin:cKO	3.84 ± 0.24	20.82 ± 0.53

Fig. S5. IdU/BrdU dual labeling for estimating the lengths of the S-phase and total cell cycle. (**A**) An antibody specific to BrdU failed to label IdU incorporated cells (green) in the absence of BrdU injection. (**B**) A pulse of IdU was followed by a pulse of BrdU 3 hours later that could be distinguished using an antibody that recognizes both BrdU and IdU (green), and one that is specific to BrdU (red). (**C**) Representative confocal micrographs of IdU (green) and BrdU (red) labeled nuclei in P21 cWT and Nestin:cKO SEZs. Red dots highlight IdU+/BrdU+ cells. (**D**) Estimated lengths of S (Ts) and total cell cycle (Tc) in the P0 and P21 wild-type and mutant SEZ progenitors. Data are mean±s.e.m., *n*=3/genotype/age.

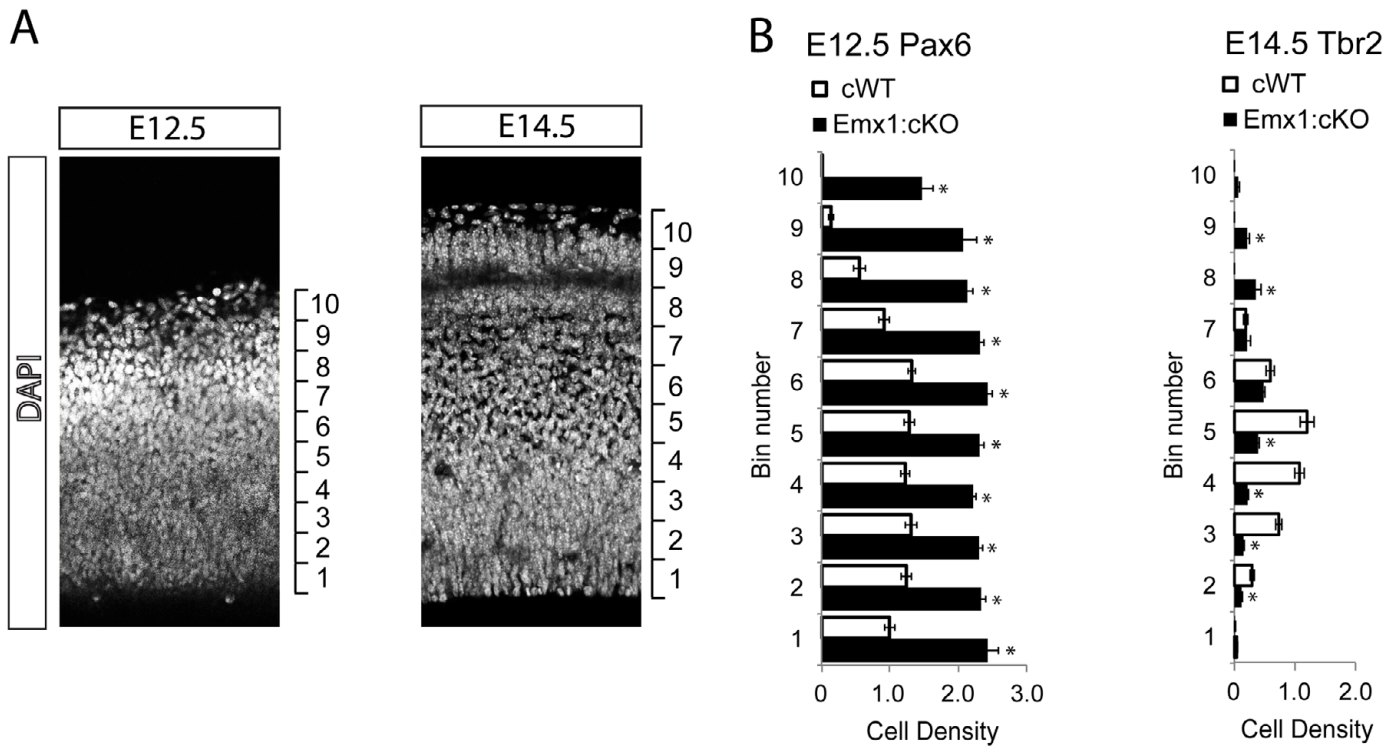

Fig. S6. Distribution of Pax6 and Tbr2 progenitors in the E12.5 and E14.5 cerebral cortex. (**A**) The thickness of E12.5 and E14.5 cerebral cortices were visualized by DAPI nuclear staining and divided into 10 equidistant bins to quantify distribution of distinct makers. (**B**) Quantified densities of Pax6+ or Tbr2+ cells in each bin of Emx1:cWT and Emx1:cKO cerebral cortices at each age. Data are mean±s.e.m.; **P*<0.01, Student's *t*-test, n=3/age group/genotype.

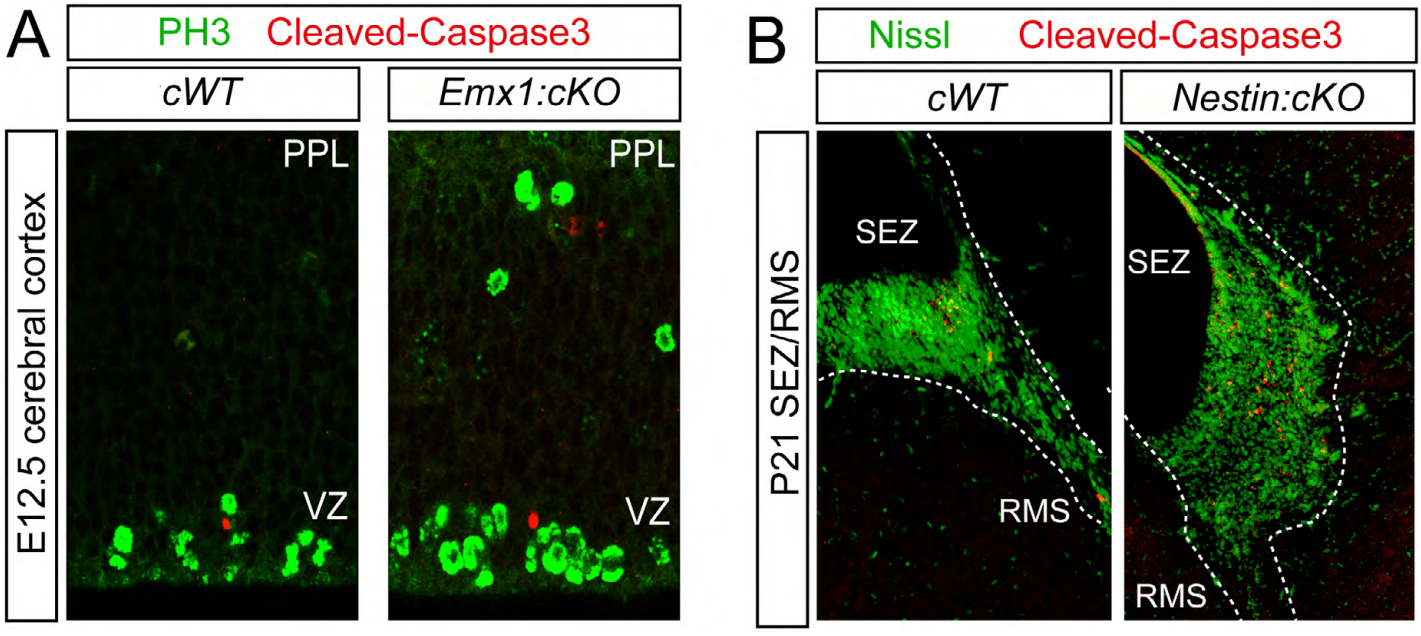

Fig. S7. Analysis of caspase-dependent apoptosis in conditionally Sp2-deleted embryonic cerebral cortex and postnatal SEZ/RMS. (**A**) Confocal images of tissue stained for cleaved caspase 3 (red) and PH3 (green) in the E12.5 cerebral cortex. The density and distribution of cleaved caspase 3-labeled apoptotic cells were indistinguishable in *Emx1:cWT* and *Emx1:cKO* cortices. (**B**) At P21, an increase in immunoreactivity for cleaved-caspase 3 (red) emerged within the cellular bulge revealed by Nissl stain (green) in Nestin:cKO compared with cWT SEZ and RMS.

Table S1. Mice purchased from the Jackson laboratory

Name	Jackson Laboratory ID	Catalogue #
Nestin-cre	B6.Cg-*Tg (Nes-cre)1Kln*/J	003771
tdTomato	B6.129S6-*Gt (ROSA) 26Sor*$^{tm14\ (CAG-tdTomato)\ Hze}$/J	007908
Emx1^{cre}	B6.129S2-*Emx1*$^{tm1(cre)Krj}$/J	005628

Antibody	Source	Dilution
rabbit anti-Ki67	Vision Biosystems	1:500
rabbit anti-PH3	Millipore	1:500
mouse anti- PH3	Abcam	1:500
mouse anti-BrdU	BD Bioscience	13:1000
guinea pig anti-Dcx	Millipore	1:1000
mouse anti-GFAP	Millipore	1:1000
mouse anti-NeuN	Millipore	1:1000
rabbit anti-S100_	Sigma	1:1000
rabbit anti-Dlx2	Gift of Dr. David Eisenstat	1:1000
rabbit anti-Gsx2	Gift of Dr. Kenny Campbell	1:4000
rabbit anti-Pax6	Millipore	1:500
rabbit anti-cleaved caspase3	Cell Signaling	1:1000
rabbit anti-BLBP	Millipore	1:500
rabbit anti-Tbr2	Abcam	1:500
Rabbit anti-NG2	Millipore	1:1000
Mouse anti-Tuj1	Covance	1:1000
Rabbit anti-Cux1	Santa Cruz	1:500
Rabbit anti-Ctip2	Abcam	1:500
Rat anti-BrdU	Abcam	1:200
chicken anti-GFP	Abcam	1:1000
rabbit anti-RFP	Abcam	1:1000
Goat anti-rabbit Alexa488	Invitrogen	1:1000
Goat anti-mouse Alexa488	Invitrogen	1:1000
Goat anti-chicken Alexa488	Invitrogen	1:1000
Goat anti-rabbit Cy3	Millipore	1:1000
Goat anti-mouse Cy3	Millipore	1:1000
Goat anti-rabbit Alexa647	Invitrogen	1:500
Goat anti-mouse Alexa647	Invitrogen	1:500
Goat anti-guinea pig Cy3	Millipore	1:1000

Table S2. Primary and secondary antibodies used in the study.